

# Predicting the activity of amorphous catalyst sites and supported nanoparticle stability via first-principles

By Bryan R. Goldsmith



**CHEMICAL ENGINEERING**  
**UC SANTA BARBARA**

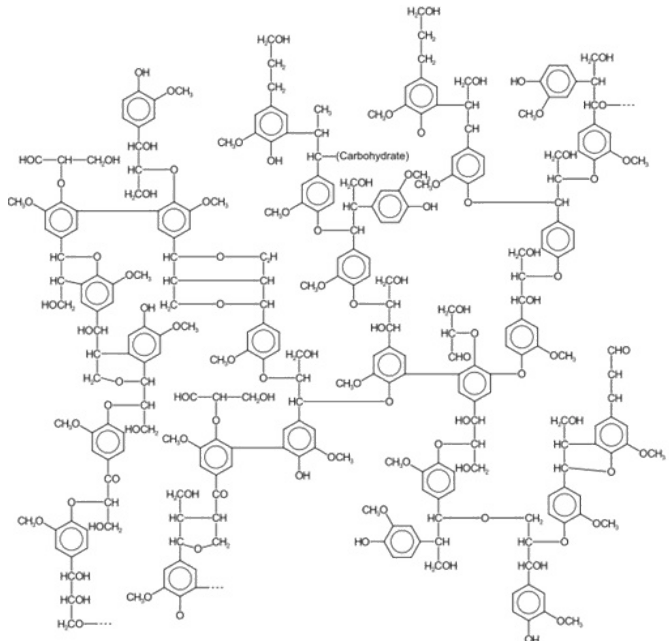


The Peters Group



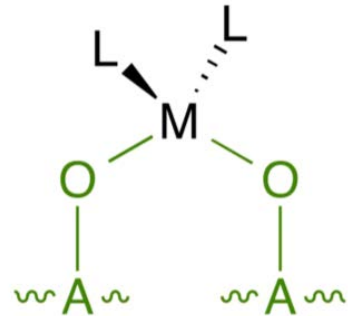
*science crossing borders...*

# Catalysis is a multibillion-dollar industry

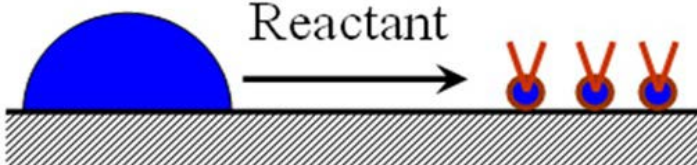


# Towards understanding the synthesis, activity, and stability of catalysts

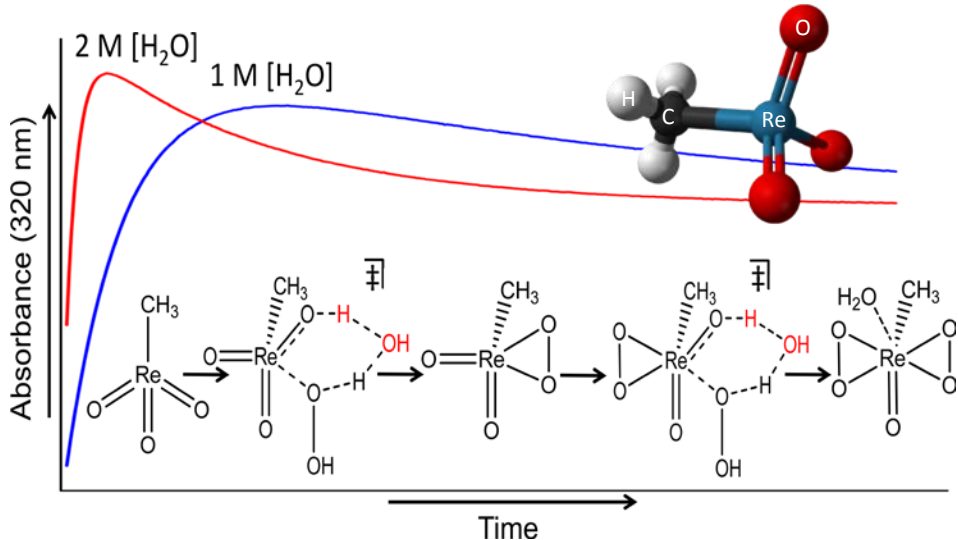
Modeling quenched disorder of catalyst sites on amorphous supports



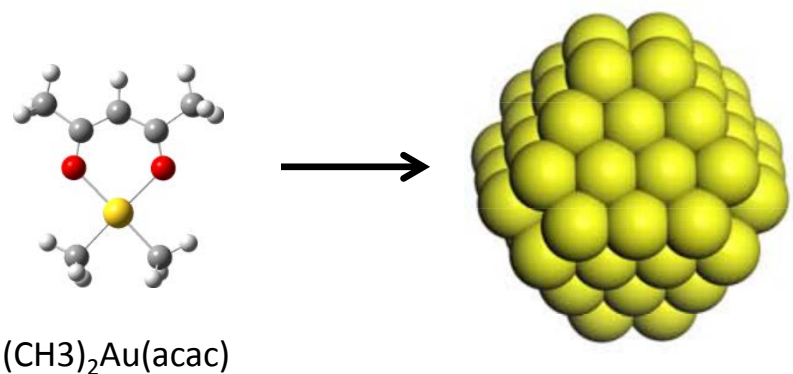
Predicting the stability of supported nanoparticles



Kinetics of homogeneous catalysts

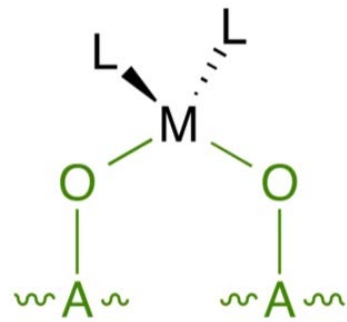


Nucleation & growth of nanoparticles

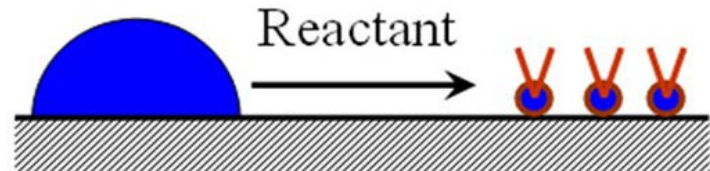


# Applying modeling to understand the synthesis, activity, and stability of catalysts

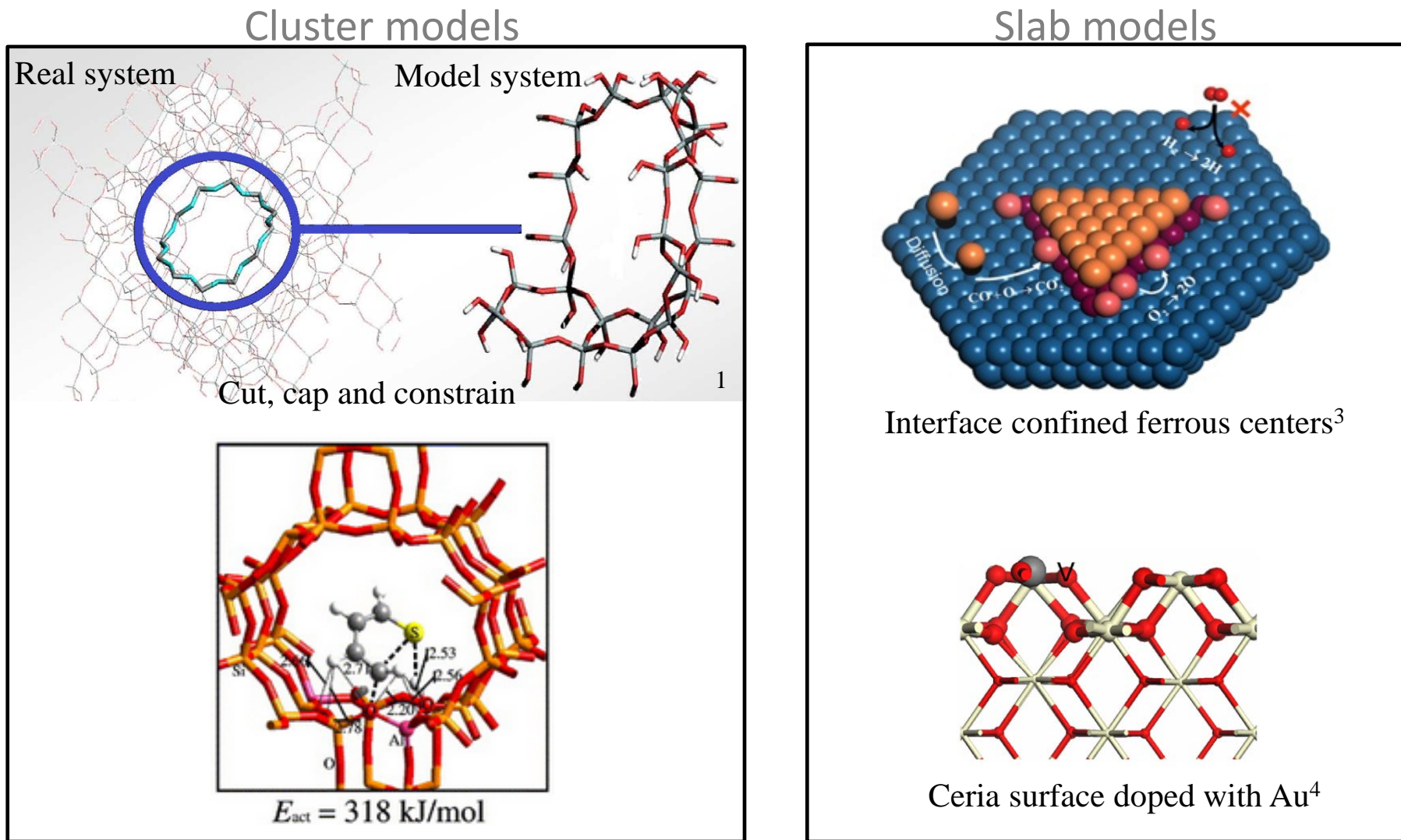
Modeling quenched disorder of catalyst sites on amorphous supports



Predicting the stability of supported nanoparticles



# Catalysis by crystalline materials: from structure to properties



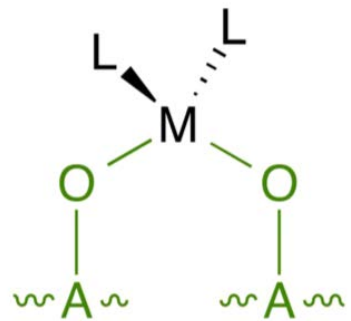
1. British Zeolite Association webpage <http://www.bza.org/>

2. X. Rozanska et.al., J. Catal., 2002, 388

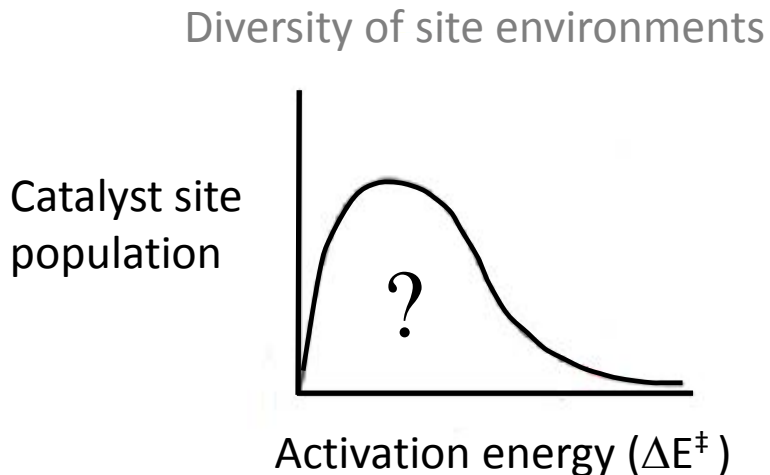
3. Q. Fu et. al. Science 328, 2010, 1141

4. Nolan et al. Surface Science. 2008, 602, 2374

# Modeling amorphous catalysts has been an intractable problem



Cr/SiO<sub>2</sub>  
Cr/AlPO<sub>4</sub>  
CH<sub>3</sub>ReO<sub>3</sub>/silica-alumina  
Mo/SiO<sub>2</sub>  
Ti/SiO<sub>2</sub>  
Ta/SBA15



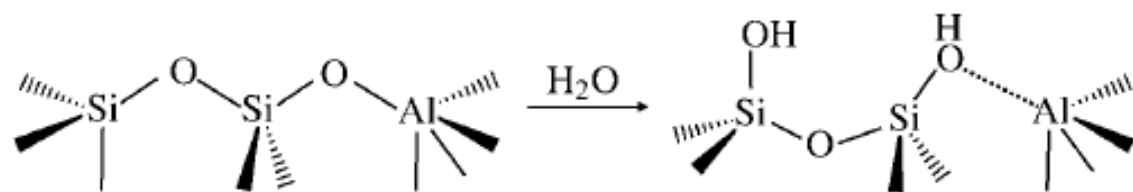
Many reasons to try

- Some catalysts only work on amorphous supports
- Unknown initiation mechanism
- How do typical dead sites and active sites differ?

Drawings specify topology, but activity also depends on site environment



Ruddy and Tilley, JACS, 130, 11088 (2008)



Chizallet and Raybaud, Angew. Chem. 48, 2891 (2009)

# Single atom catalysts on amorphous supports: a quenched disorder perspective

Rate for site geometry  $\mathbf{x}$

$$k(\mathbf{x}) = A(\mathbf{x}) \exp[-\beta \Delta E(\mathbf{x})]$$

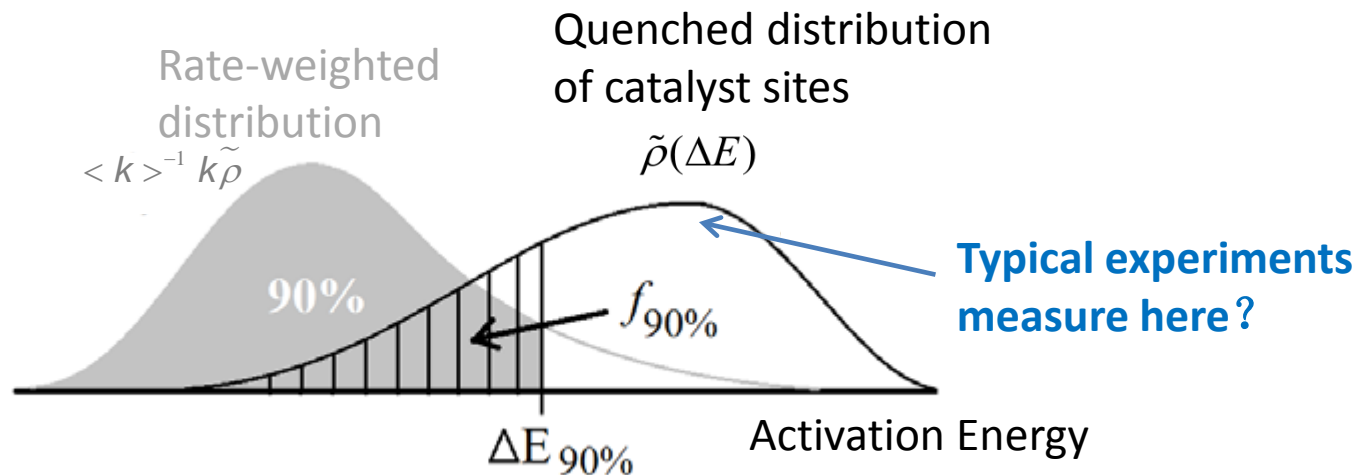
$$\langle k \rangle = \int d\mathbf{x} k(\mathbf{x}) \rho(\mathbf{x})$$

Project to activation energy distributions

$$\tilde{\rho}(\Delta E) \equiv \int d\mathbf{x} \rho(\mathbf{x}) \delta[\Delta E - \Delta E(\mathbf{x})]$$

$$k(\Delta E) \equiv \tilde{\rho}(\Delta E)^{-1} \int d\mathbf{x} \rho(\mathbf{x}) k(\mathbf{x}) \delta[\Delta E - \Delta E(\mathbf{x})]$$

$$\langle k \rangle = \int d\Delta E k(\Delta E) \tilde{\rho}(\Delta E)$$



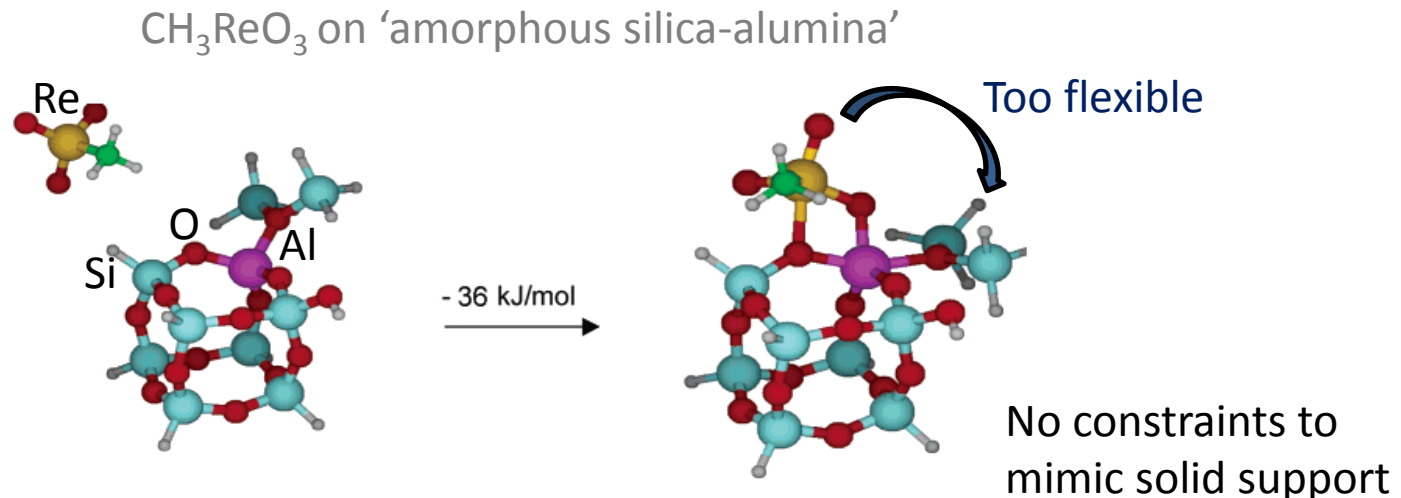
Kinetics are highly sensitive to the low energy tail

New methods are needed to sample the most reactive sites

# Typical modeling protocols for amorphous materials

Often necessary to make undesirable assumptions

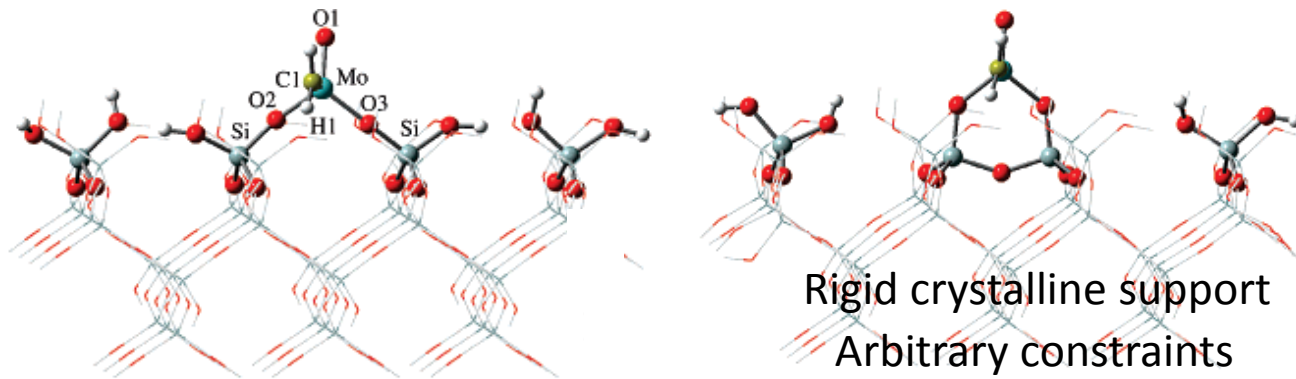
Use an approximate support and model in the gas phase



# Typical modeling protocols for amorphous materials

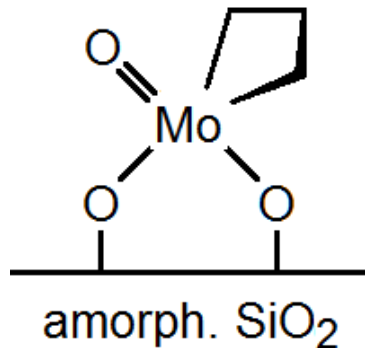
Use a crystalline support with rigid constraints

Mo/Silica catalyst cut from  $\beta$ -cristobalite



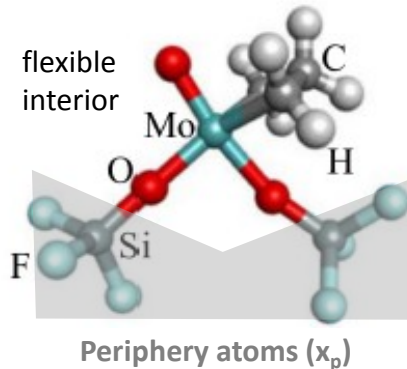
two out of 10 different models tested

# Our approach to modeling isolated catalyst sites on amorphous supports

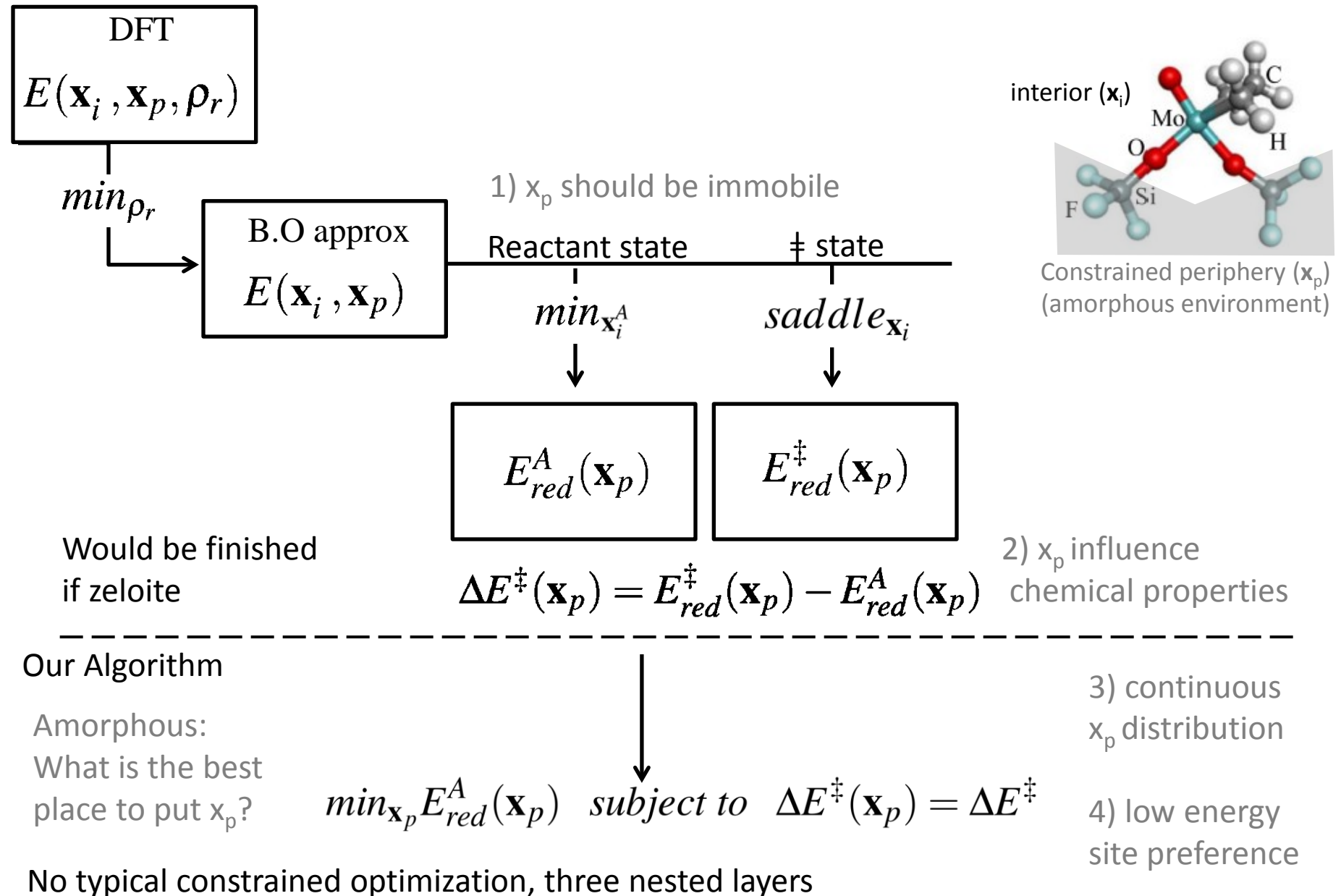


## Modeling premises

- 1) Periphery atoms ( $x_p$ ) should be immobile
- 2) Periphery atoms influence chemical properties of the site
- 3) Periphery atoms arranged in an *unknown and continuous distribution*
- 4) For any  $\Delta E^\ddagger(x_p)$ , assume low energy sites prevalent



# Connecting our algorithm to usual zeolite modeling approach

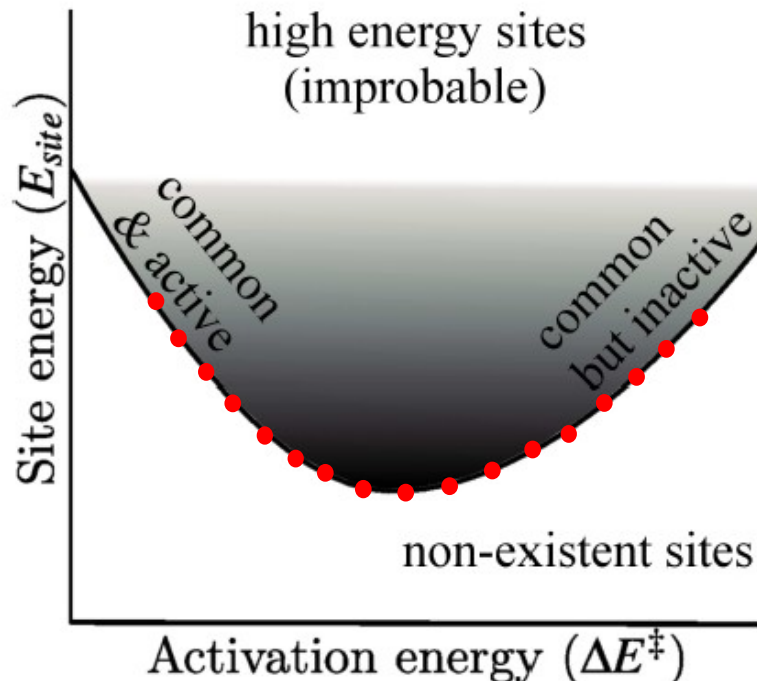


# From properties to structures, instead of from structures to properties

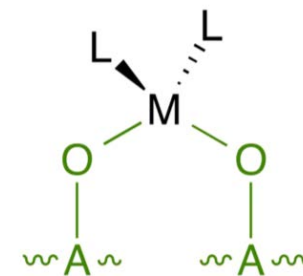
$$\min_{\mathbf{x}_p} E_{red}^A(\mathbf{x}_p) \text{ subject to } \Delta E^\ddagger(\mathbf{x}_p) = \Delta E^\ddagger$$

Use Sequential Quadratic Programming

Generates low energy catalyst structures  
with varying degrees of reactivity



Each point on curve thought of as a different catalyst site



Different anchor point, A

# Algorithm Formulation

Local quadratic expansion

$$E(\mathbf{x}_i^A + \Delta\mathbf{x}_i^A, \mathbf{x}_p + \Delta\mathbf{x}_p) - E(\mathbf{x}_i^A, \mathbf{x}_p) =$$

$$\begin{bmatrix} \Delta\mathbf{x}_i^A & \Delta\mathbf{x}_p \end{bmatrix} \begin{bmatrix} \mathbf{g}_i^A \\ \mathbf{g}_p^A \end{bmatrix} + \frac{1}{2} \begin{bmatrix} \Delta\mathbf{x}_i^A & \Delta\mathbf{x}_p \end{bmatrix} \begin{bmatrix} H_{ii}^A & H_{ip}^A \\ H_{pi}^A & H_{pp}^A \end{bmatrix} \begin{bmatrix} \Delta\mathbf{x}_i^A \\ \Delta\mathbf{x}_p \end{bmatrix}$$

Similarly for transition state

Minimize  $E(\mathbf{x}_i^A, \mathbf{x}_p)$  given any  $\Delta\mathbf{x}_p$  by interior optimization

$$\underline{\Delta\mathbf{x}_i^A = -(H_{ii}^A)^{-1}(\mathbf{g}_i^A + H_{ip}^A \Delta\mathbf{x}_p)}$$

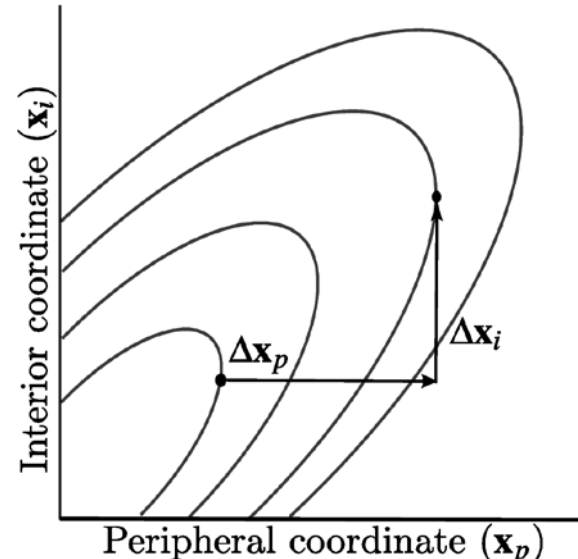
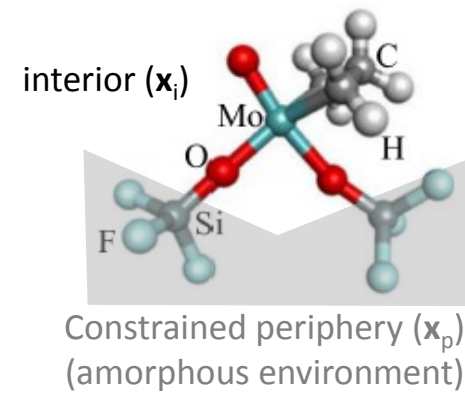
Optimize interior atoms for given  $\Delta\mathbf{x}_p$

Move periphery atoms

Similarly for transition state

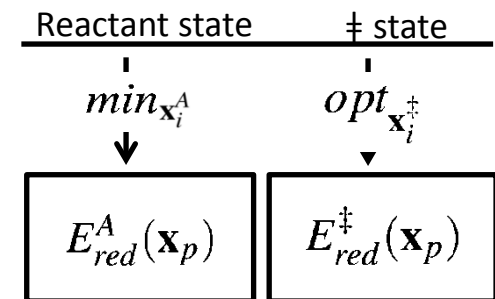
Key

Reactant state - superscript A  
gradient vector -  $\mathbf{g}$   
Hessian matrix -  $\mathbf{H}$   
Interior coordinate -  $\mathbf{x}_i$   
Periphery coordinate -  $\mathbf{x}_p$



## Reduced potential energy surface

$$E_{red}^A(\mathbf{x}_p + \Delta\mathbf{x}_p) = E_{red}^A(\mathbf{x}_p) + (\Delta\mathbf{x}_p)^T \mathbf{g}_{red}^A + \frac{1}{2} (\Delta\mathbf{x}_p)^T H_{red}^A \Delta\mathbf{x}_p$$



Find the lowest energy sites with a given activation energy

$$\min_{\mathbf{x}_p} E_{red}^A(\mathbf{x}_p) \text{ subject to } \Delta E^\ddagger(\mathbf{x}_p) = \Delta E^\ddagger$$

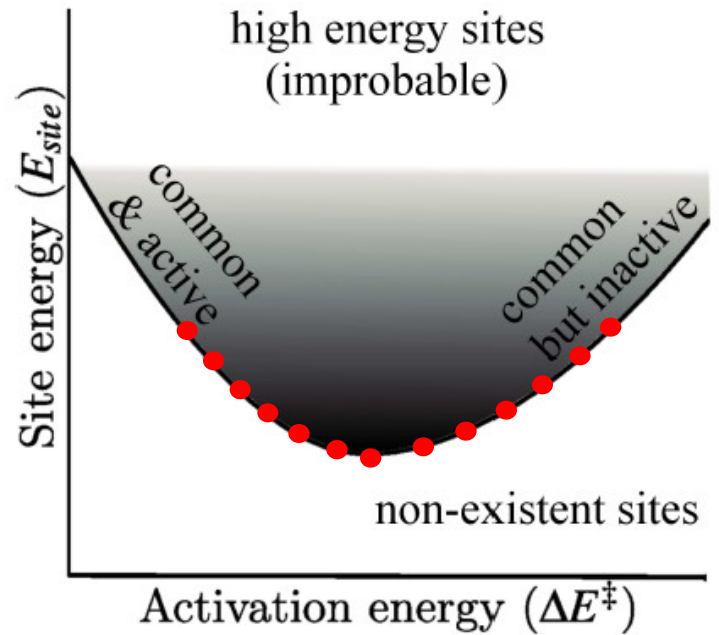
↓  
Sequential Quadratic  
Programming

'Dial' the activation energy

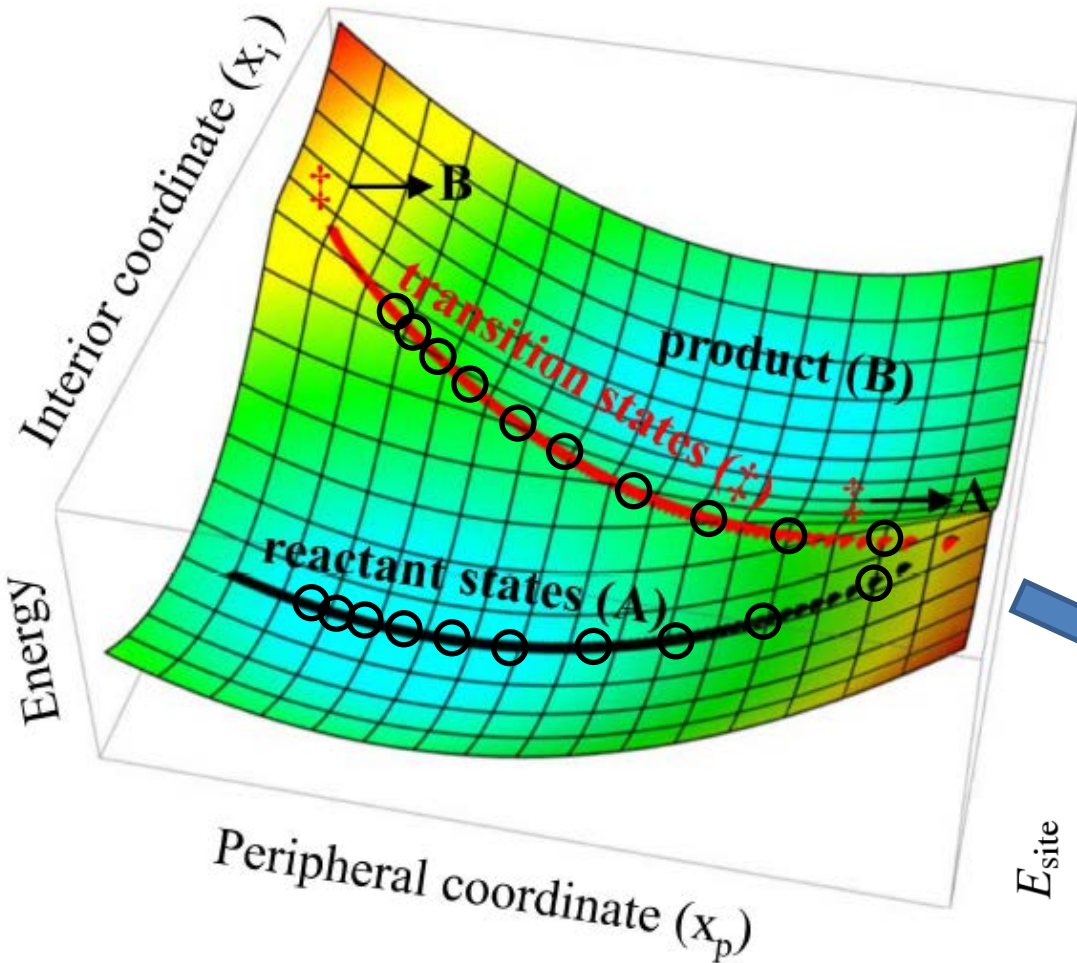
$$\Delta\mathbf{x}_p \leftarrow \Delta\Delta E^\ddagger$$

New catalyst site  
structure

Step in  
activation energy



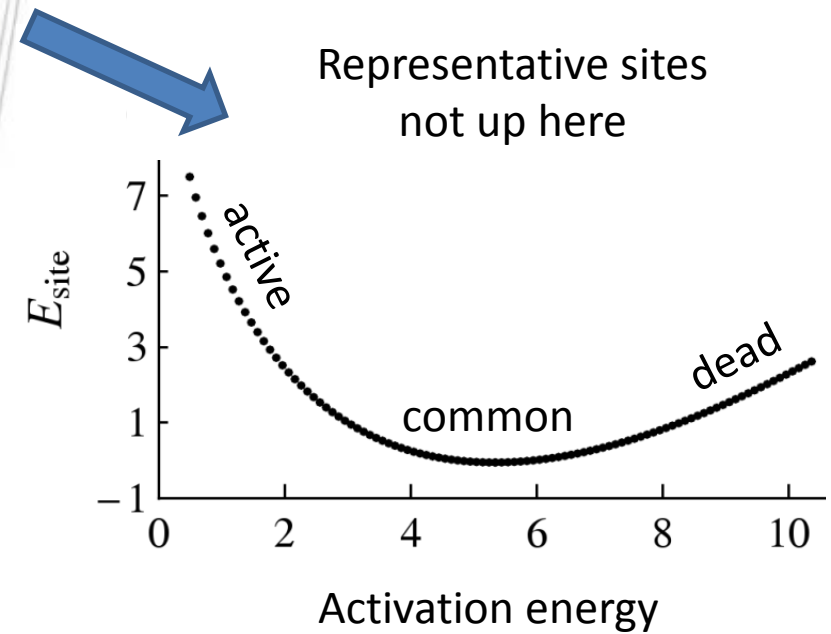
# Example: Empirical Valence Bond Model Energy Landscape



$$\Delta \mathbf{x}_p = -(H_{red}^A)^{-1}(\mathbf{g}_{red}^A - \lambda \Delta \mathbf{g}_{red}).$$

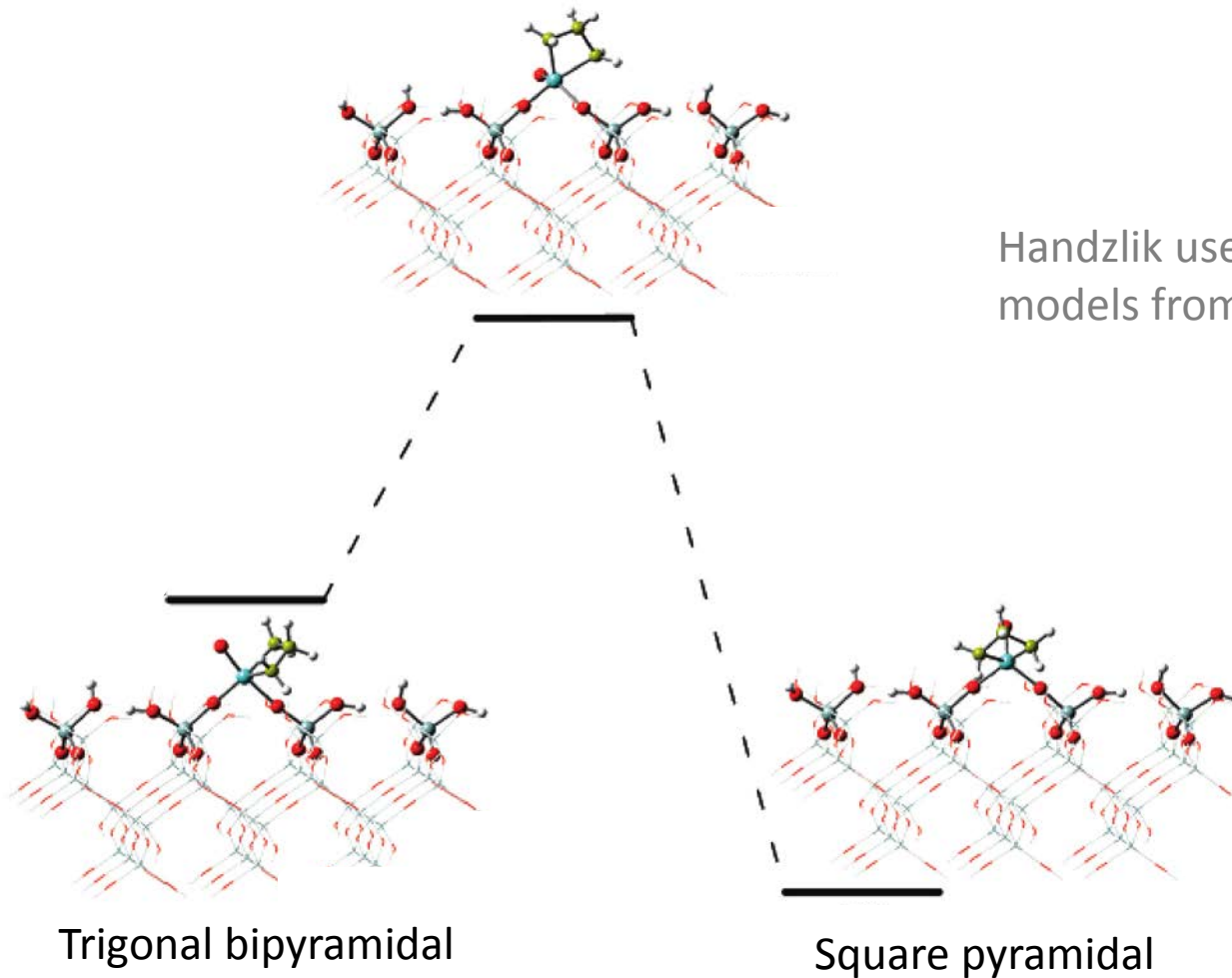
$$\lambda = \frac{\Delta \Delta E^\ddagger + (\Delta \mathbf{g}_{red})^T (H_{red}^A)^{-1} \mathbf{g}_{red}^A}{(\Delta \mathbf{g}_{red})^T (H_{red}^A)^{-1} \Delta \mathbf{g}_{red}}.$$

How do typical active and dead sites differ?



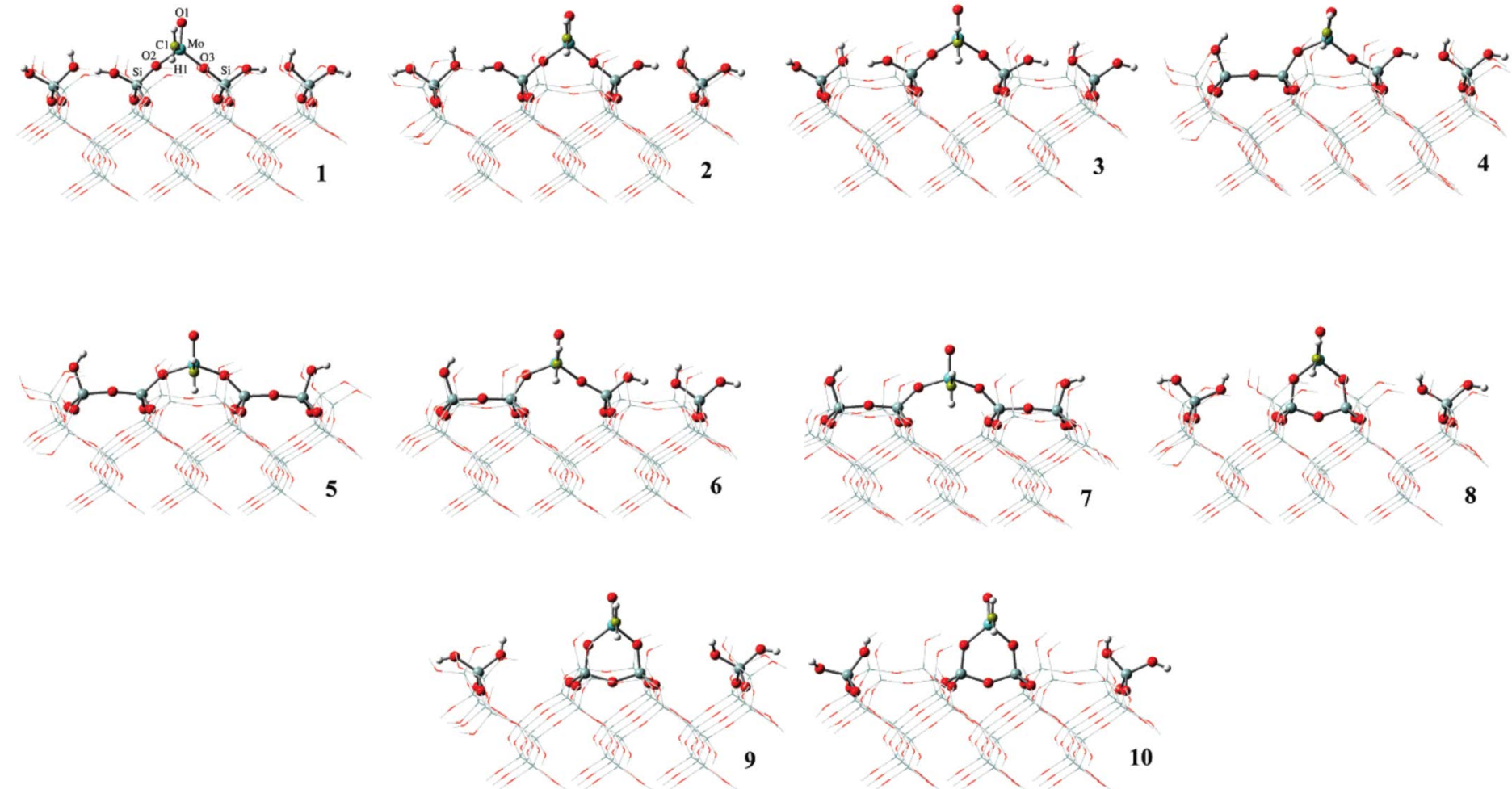
# Off-pathway intermediate formation during ethene metathesis by isolated Mo(VI) on amorphous SiO<sub>2</sub>

Metallacycle rotation

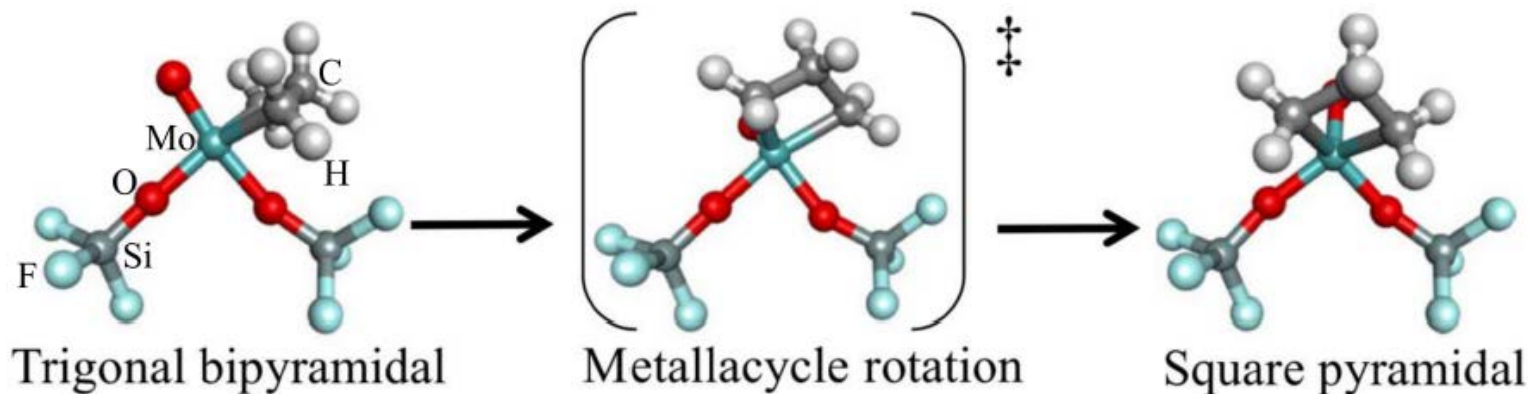


Handzlik used *ten* QM/MM models from  $\beta$ -cristobalite

# Handzlik's ten ONIOM models from $\beta$ -cristobalite

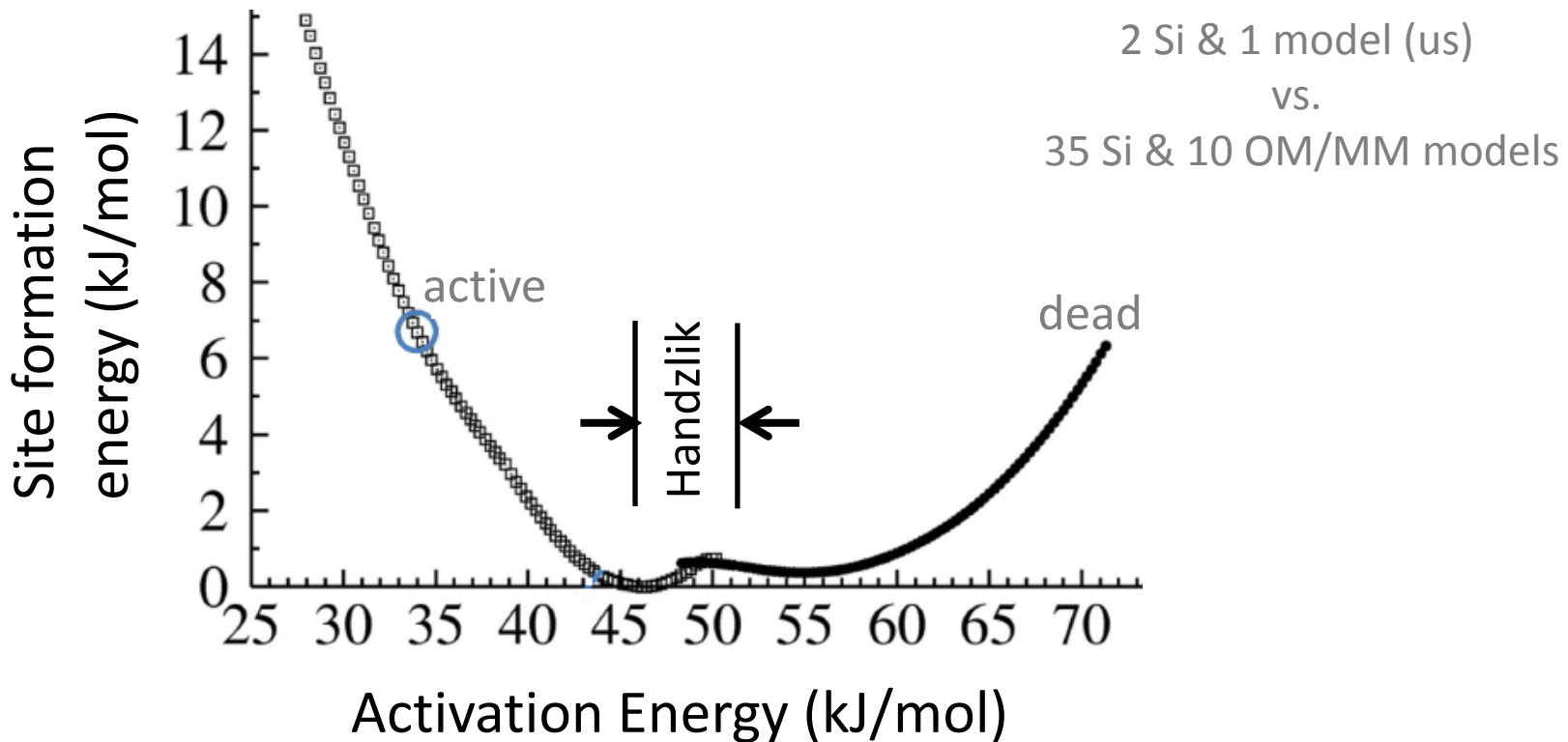
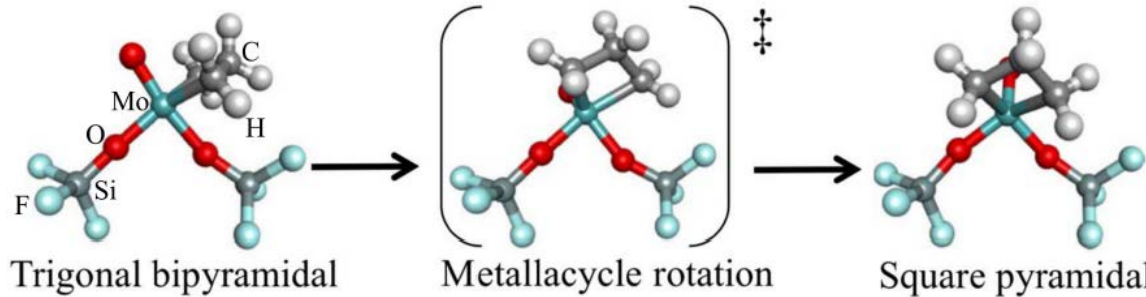


# Our quadratic programming approach to model distribution of molybdenum sites on silica



periphery: terminal F atoms  
*basis deficient to mimic OH*  
interior: everything else

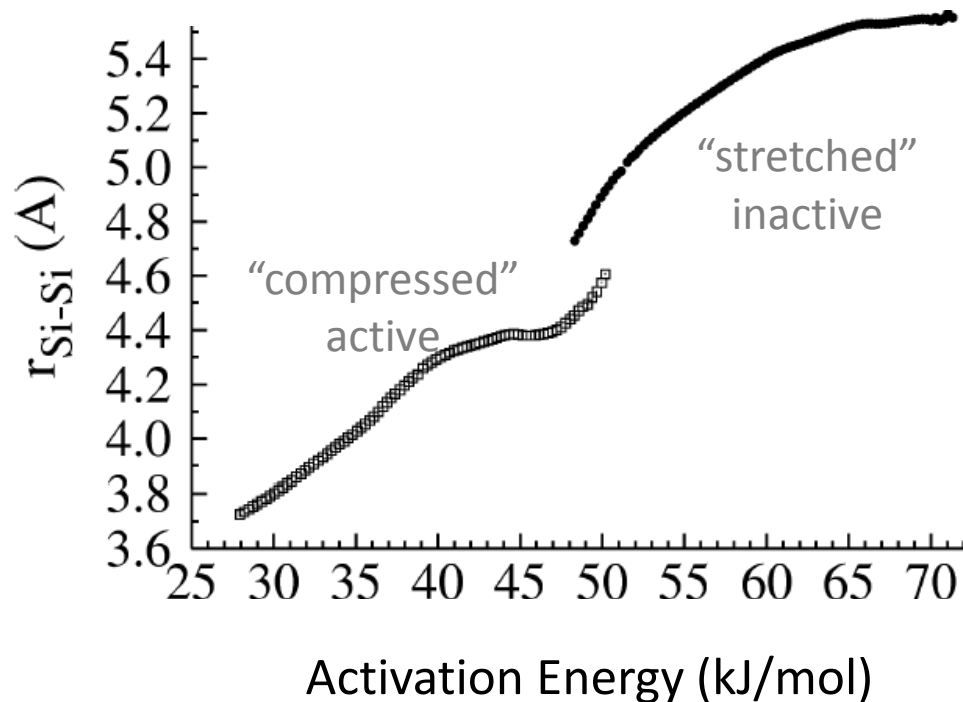
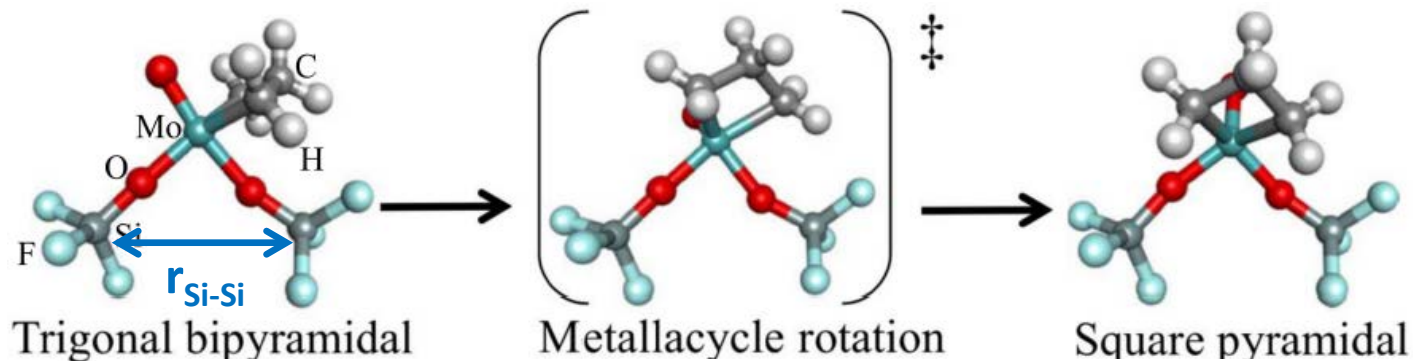
# A broad distribution of active site structures are generated



B. R. Goldsmith, E. D. Sanderson, D. Bean, B. Peters, *J. Chem. Phys.* 138, 204105 (2013)

B. R. Goldsmith *et al.* in Reaction Rate Constant Computations: Theories and Applications, The Royal Society of Chemistry (2013). Cambridge, U.K.

# Identify structural descriptors of activity

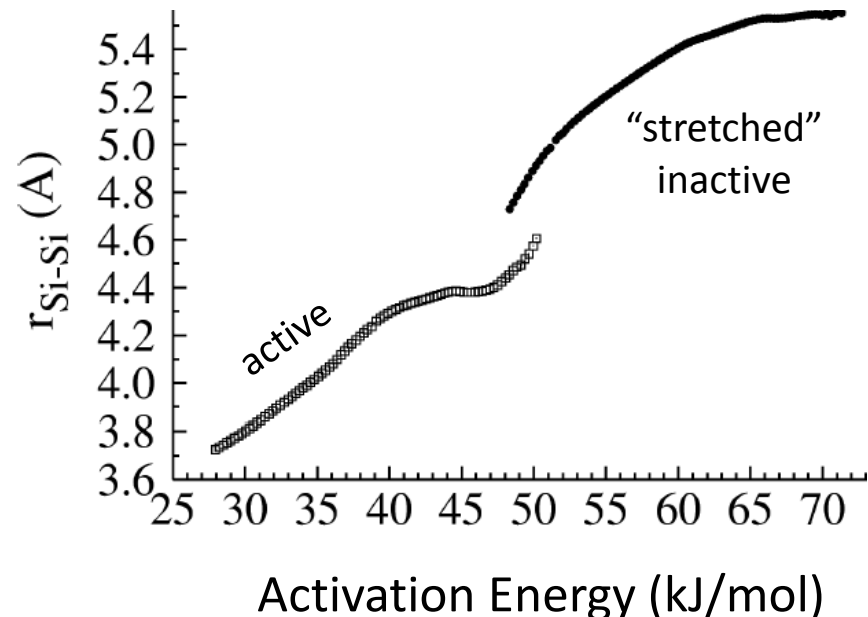
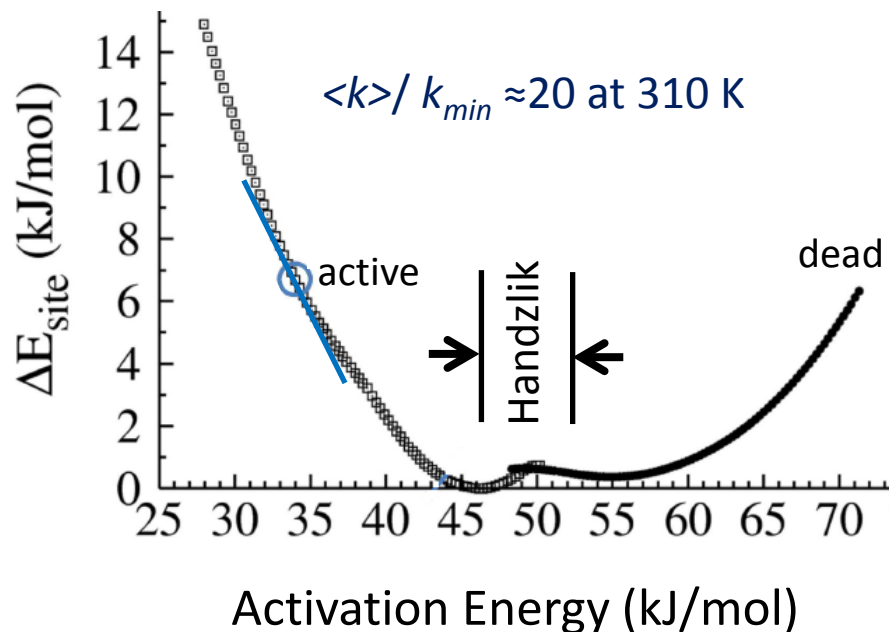


# New framework for modeling amorphous catalyst sites

From properties to structures

Generate sites with different reactivity  
Examine structure sensitivity

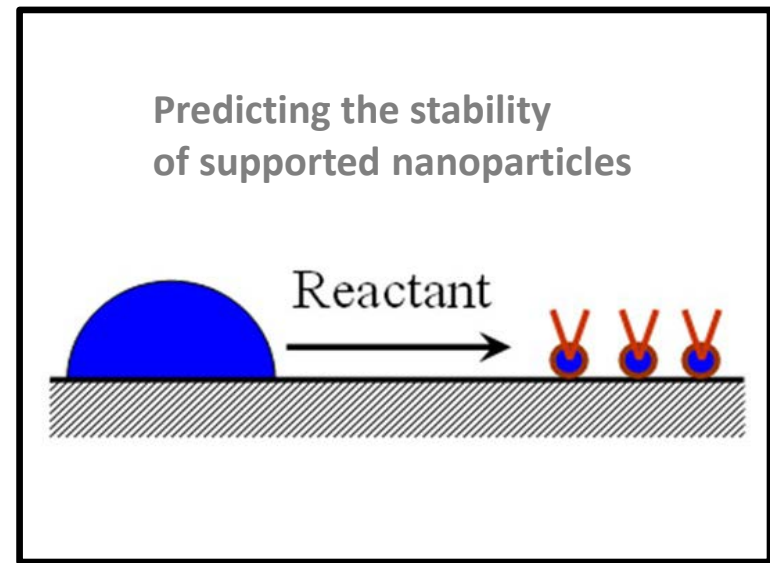
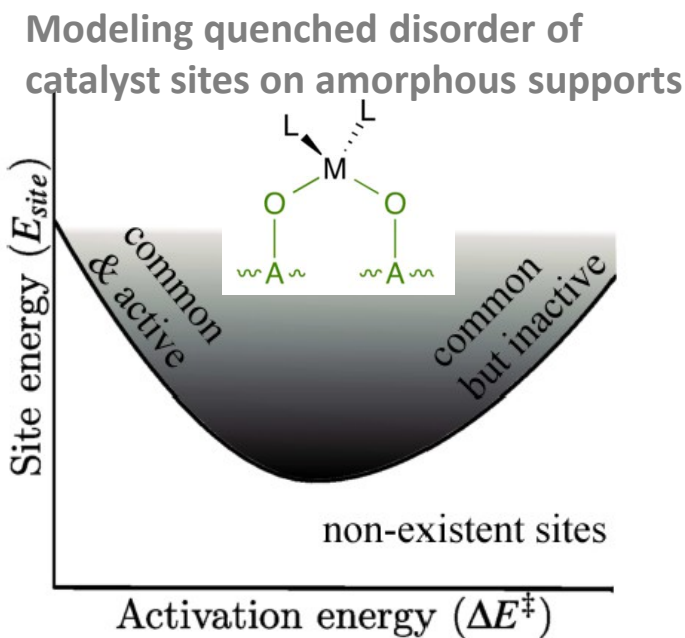
Contrast dead & active sites for descriptors



B. R. Goldsmith, E. D. Sanderson, D. Bean, B. Peters, *J. Chem. Phys.* 138, 204105 (2013)

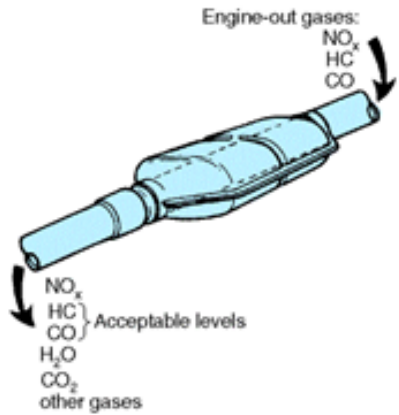
B. R. Goldsmith *et al.* in Reaction Rate Constant Computations: Theories and Applications, The Royal Society of Chemistry (2013). Cambridge, U.K.

# Applying modeling to understand the synthesis, activity, and stability of catalysts

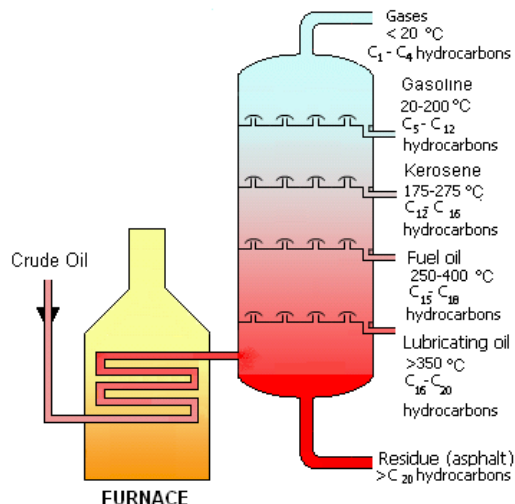


# Increasing catalyst durability and recyclability is important

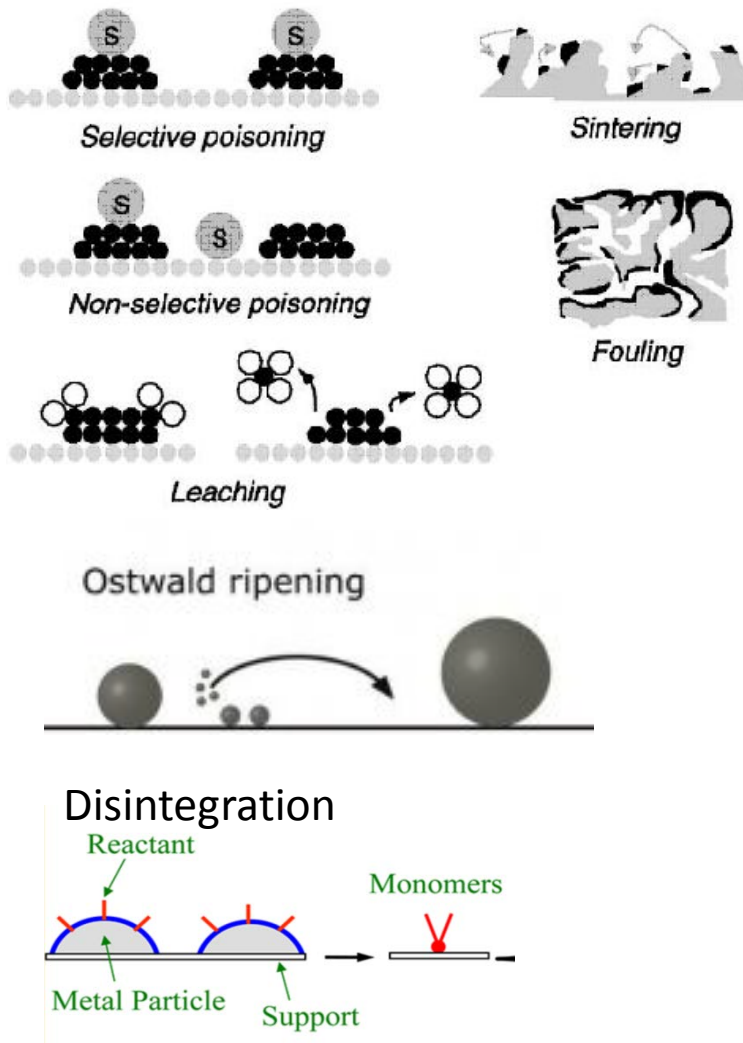
## Pollution control



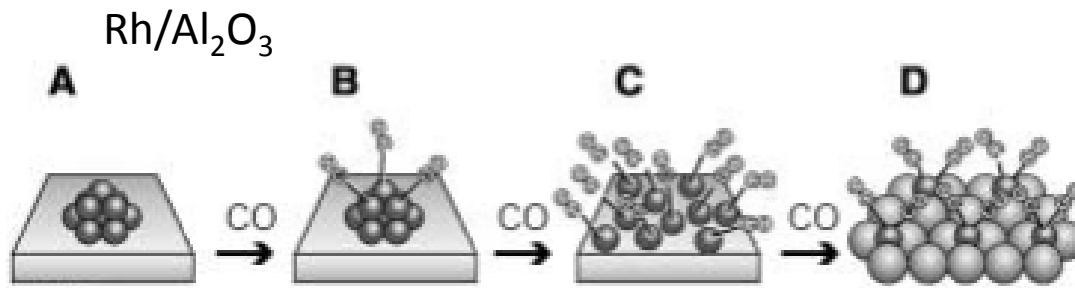
## Chemical production & alternative energy



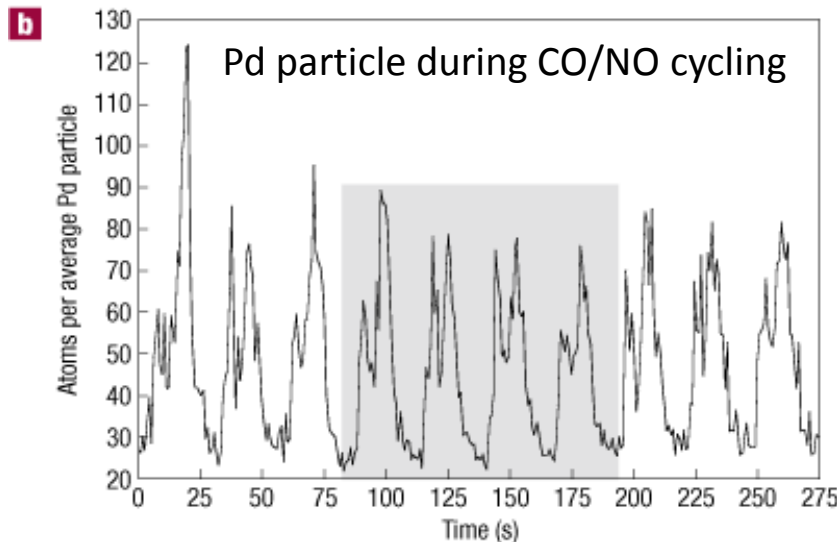
## Many modes of deactivation



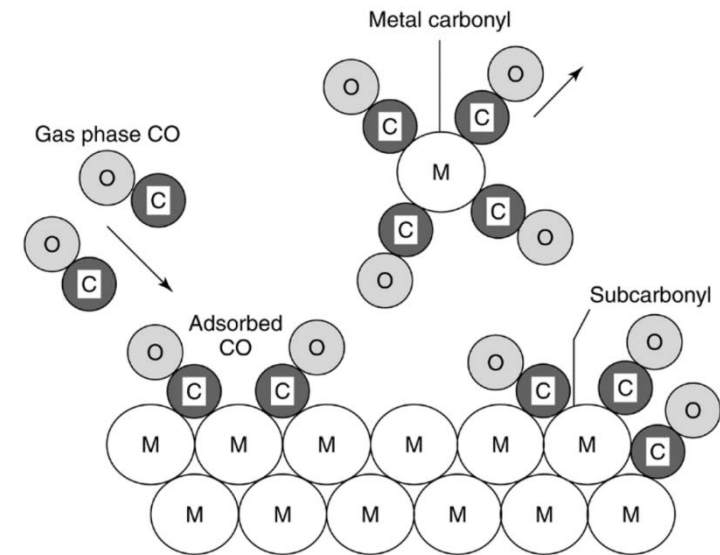
# Nanoparticle disintegration is a common phenomena



Suzuki, Angew. Chem. Int. Ed. 2003, 42, 4795 –4799



M. A. Newton,, Nat Mater 2007, 6, 528

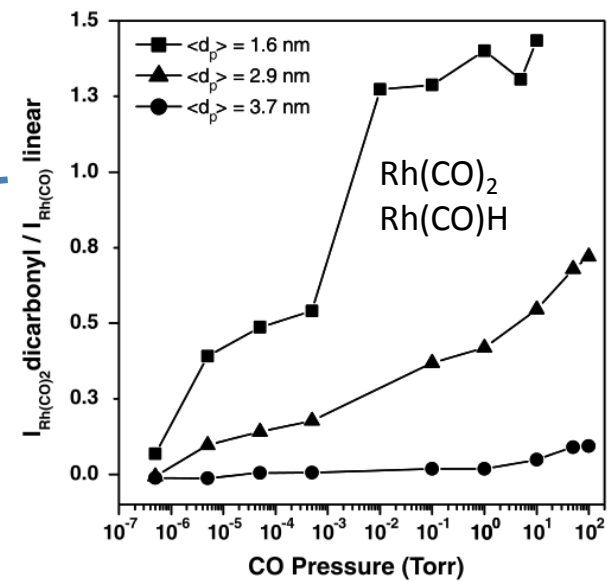
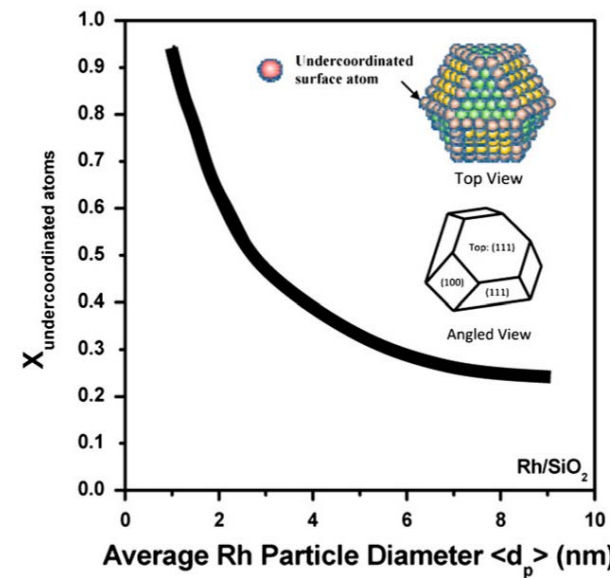
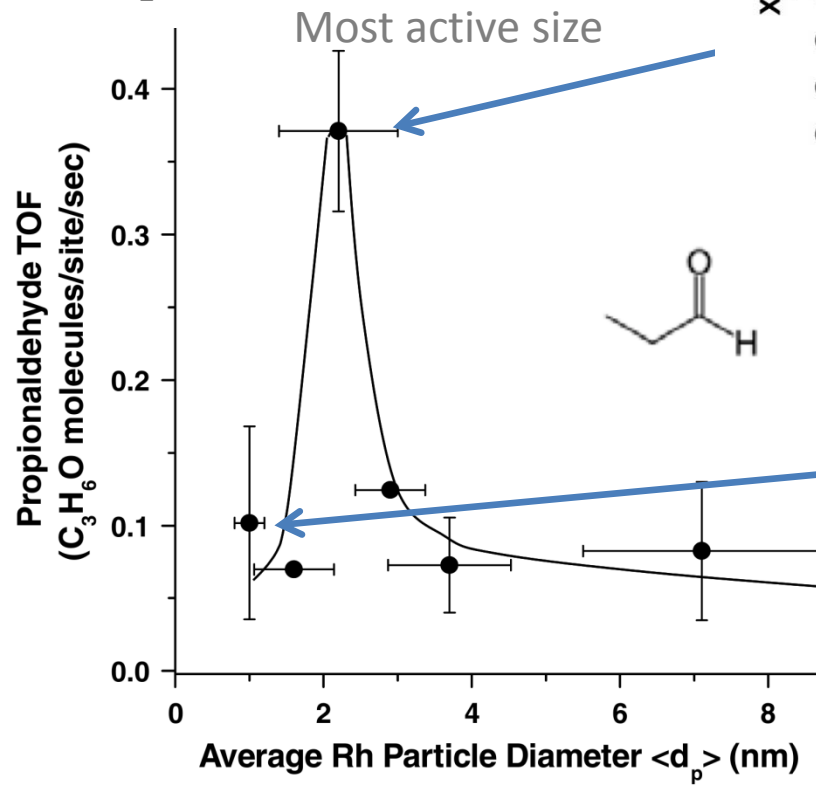


M. Argyle Catalysts 2015, 5(1), 145-269

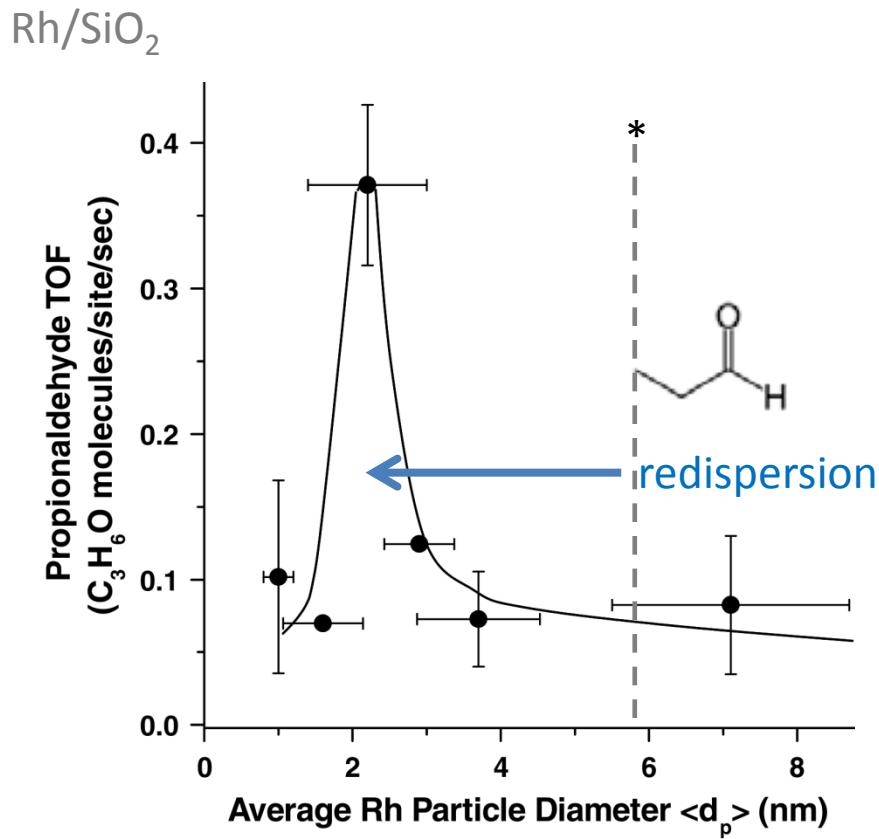
# Nanoparticle disintegration can cause catalyst deactivation



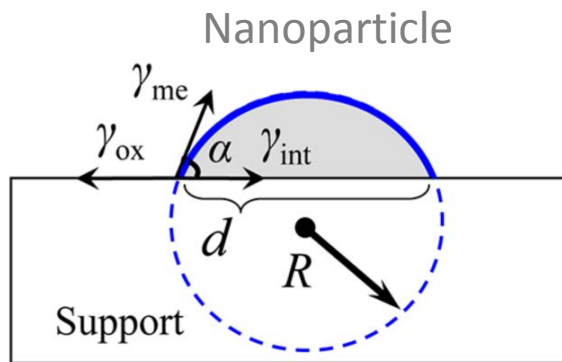
Rh/SiO<sub>2</sub>



Or, Nanoparticle disintegration  
can *redisperse agglomerated particles*



# Energetics of supported nanoparticles

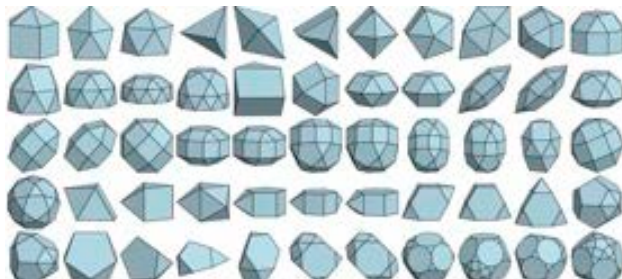


Average energy of particle per atom

$$\Delta E_{NP} = \frac{3\Omega\gamma_{me}}{R}$$

What about the effect of reactants?

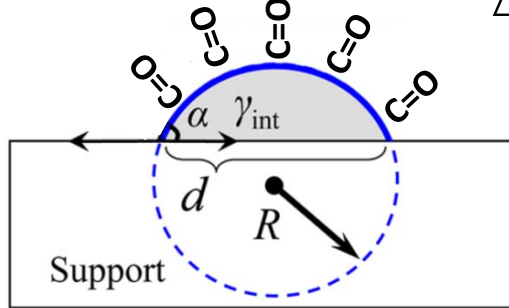
Metal nanoparticles have different exposed facets



$$\gamma_{me} = \sum_i f_i \times \gamma_i$$

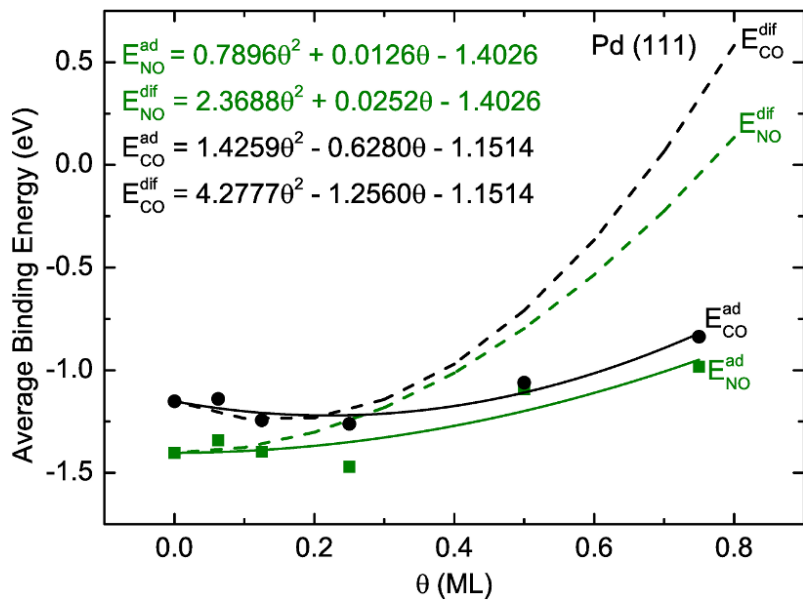
Surface energy of metal particle      Area ratio of facet i      Surface energy of facet i

# Reactant adsorption lowers particle surface energy

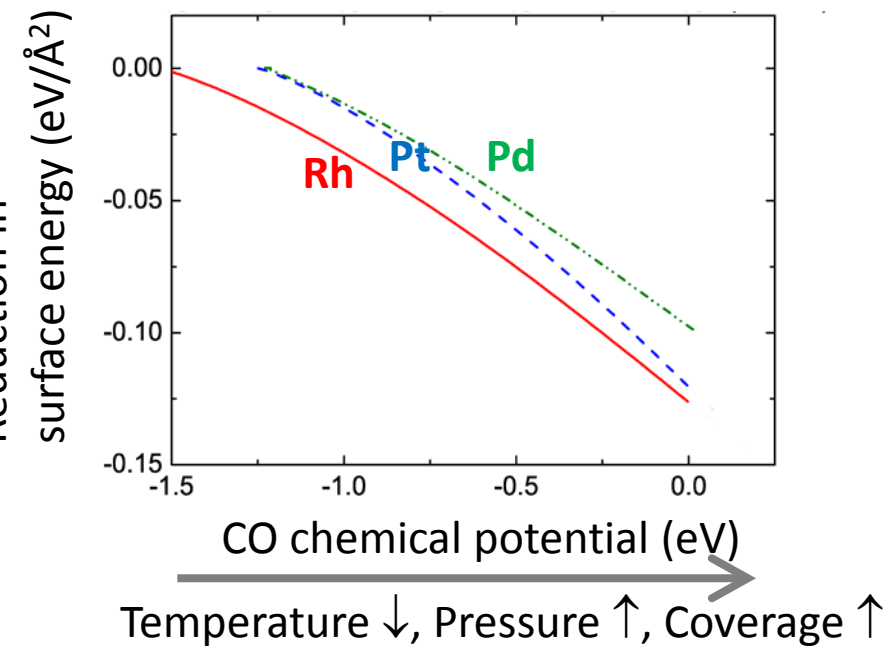


$$\Delta \bar{E}_{NP} = \frac{3\Omega \bar{\gamma}_{me}}{R} \quad \bar{\gamma}_{me} = \sum_i f_i [\gamma_i + \Delta \gamma_i(T, P)]$$

$$\Delta \gamma_i(T, P) = \frac{\theta_i [E_x^{\text{ad}}(\theta_i) - \Delta \mu_x(T, P)]}{A_i}$$

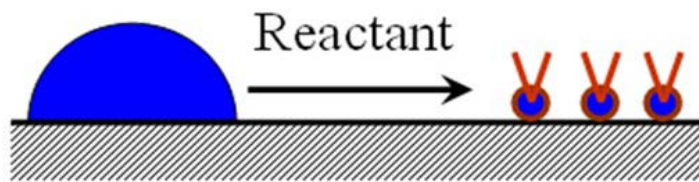


CO binding on (111) facet



# Disintegration can be modeled by the Gibbs Free Energy

$$\Delta G_{\text{disintegration}} < 0$$



Ab initio thermodynamics

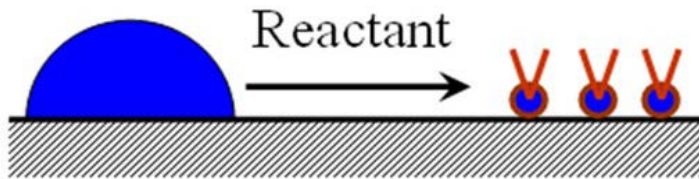
$$\Delta G_{\text{disintegration}}(R, T, p) = G_{\text{adatom-complex}} - G_{\text{reactant}} - G_{\text{n nanoparticle}}$$



Free energy of disintegration  
via adatom complex formation

# Disintegration can be modeled by the Gibbs Free Energy

$$\Delta G_{\text{disintegration}} < 0$$



Ab initio thermodynamics

$$\Delta G_{\text{disintegration}}(R, T, p) = E_f - \frac{3\Omega\bar{\gamma}_{\text{me}}}{R} - n \left[ \mu_x^0(T, p_0) + k_B T L n \frac{p_x}{p_0} \right] - TS$$

Formation energy of adatom complex

Nanoparticle energy

Standard gas phase chemical potential

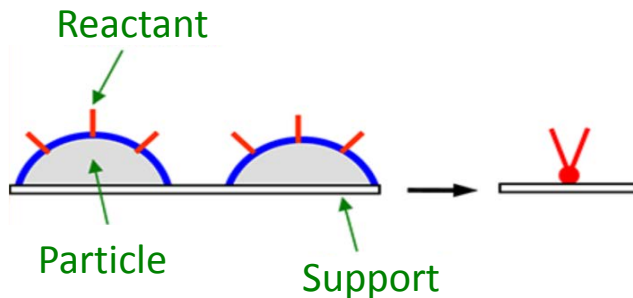
Configurational entropy of complexes

The equation shows the components of the Gibbs free energy of disintegration. The first term,  $E_f$ , is the formation energy of the adatom complex. The second term,  $\frac{3\Omega\bar{\gamma}_{\text{me}}}{R}$ , is the nanoparticle energy. The third term,  $n \left[ \mu_x^0(T, p_0) + k_B T L n \frac{p_x}{p_0} \right]$ , represents the standard gas phase chemical potential. The final term,  $-TS$ , is the configurational entropy of the complexes.

# *Ab Initio* approach to predict nanoparticle disintegration

Can we make qualitative predictions about nanoparticle disintegration that agrees with experiments?

- For supported Rh, Pd and Pt particles, which is most susceptible to disintegration?
- Among NO and CO, which one is more efficient for catalyst redispersion?
- Identify the dominant driving forces
- What are the stable species on the surface?



# Science crossing borders

UC Santa Barbara



Dalian Institute of Chemical Physics



Evan Sanderson



Prof. Wei-Xue Li



Dr. Runhai Ouyang

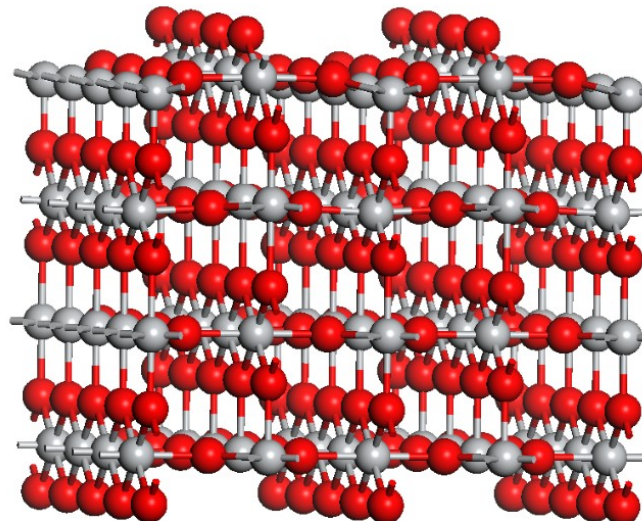
# Modeling procedure

- Projector Augmented Wave method
- RPBE Functional
- Plane wave kinetic energy cutoff = 400 eV
- Forces converged to 0.03 eV/Å
- Spin polarized



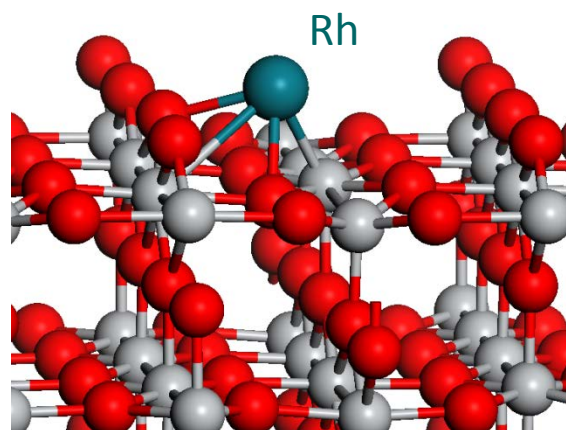
(4x2) Rutile  $\text{TiO}_2$ (110)

Periodic  
model

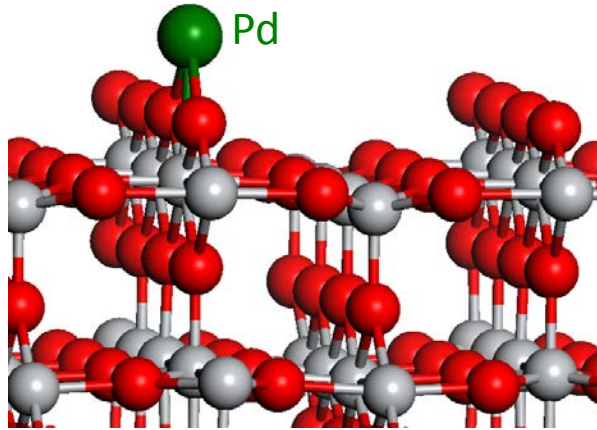


Vacuum layer  
thickness of 15 Å

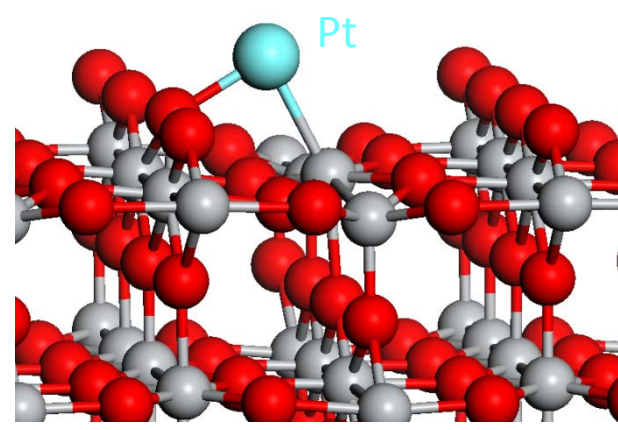
Adatom formation energies  
are large and endothermic



Formation energy = 2.88 eV



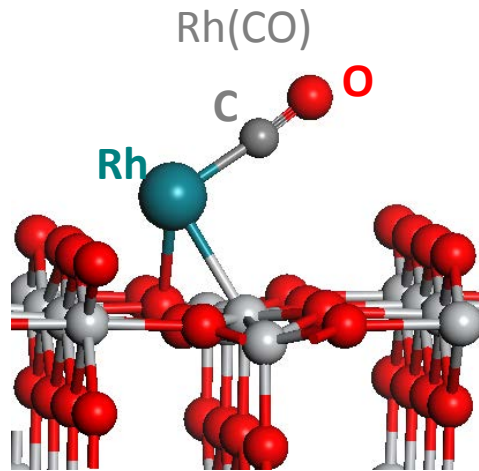
2.01 eV



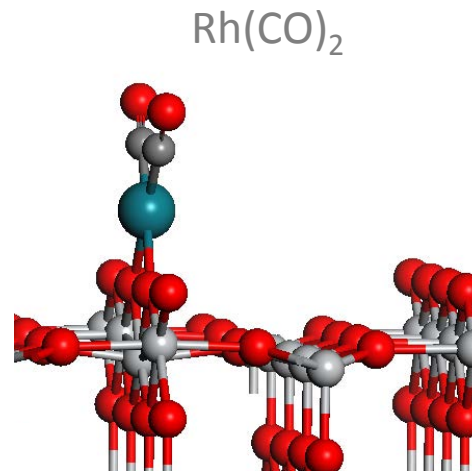
3.12 eV

$$\text{Formation energy} = E_{\text{adatom/support}} - E_{\text{support}} - E_{\text{bulk}}$$

# Reactant binding stabilizes formation of adatoms



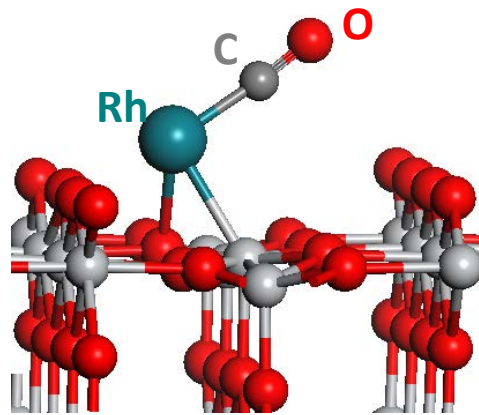
Formation energy = 0.75 eV



-1.35 eV

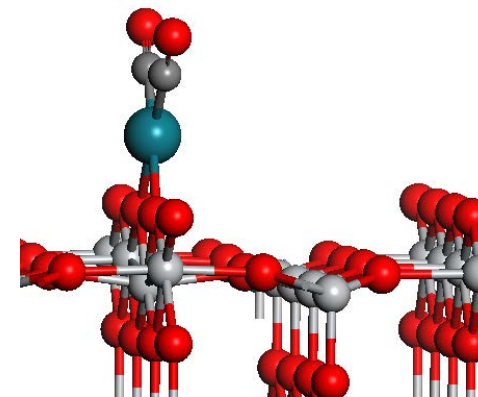
Rh(CO)<sub>2</sub> and Rh(NO)<sub>2</sub> have more favorable formation energies than Rh(CO) and Rh(NO)

Rh(CO)



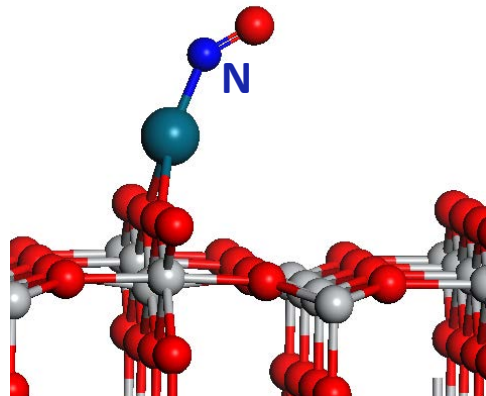
Formation energy = 0.75 eV

Rh(CO)<sub>2</sub>



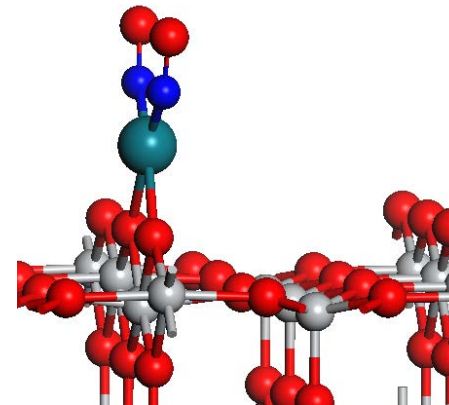
-1.35 eV

Rh(NO)



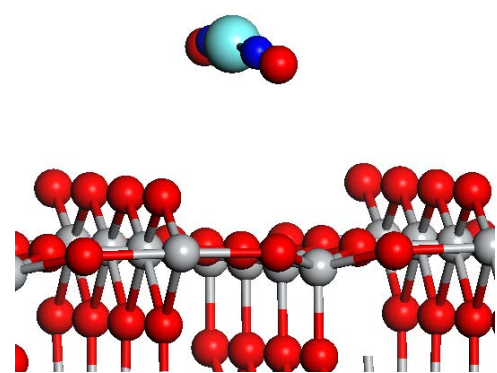
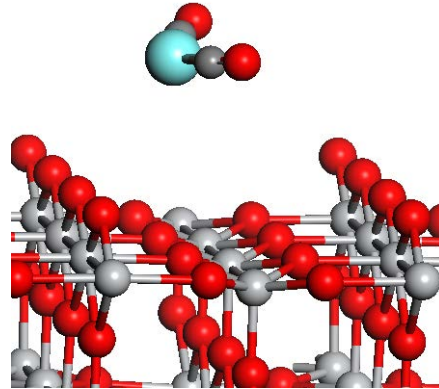
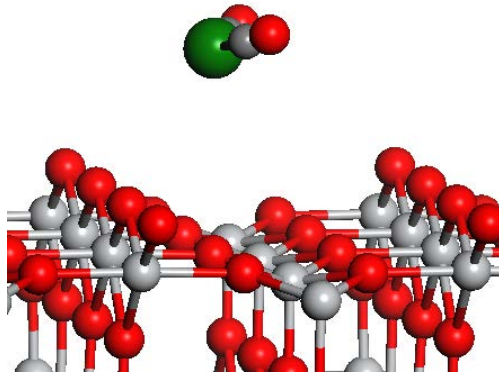
-0.02 eV

Rh(NO)<sub>2</sub>



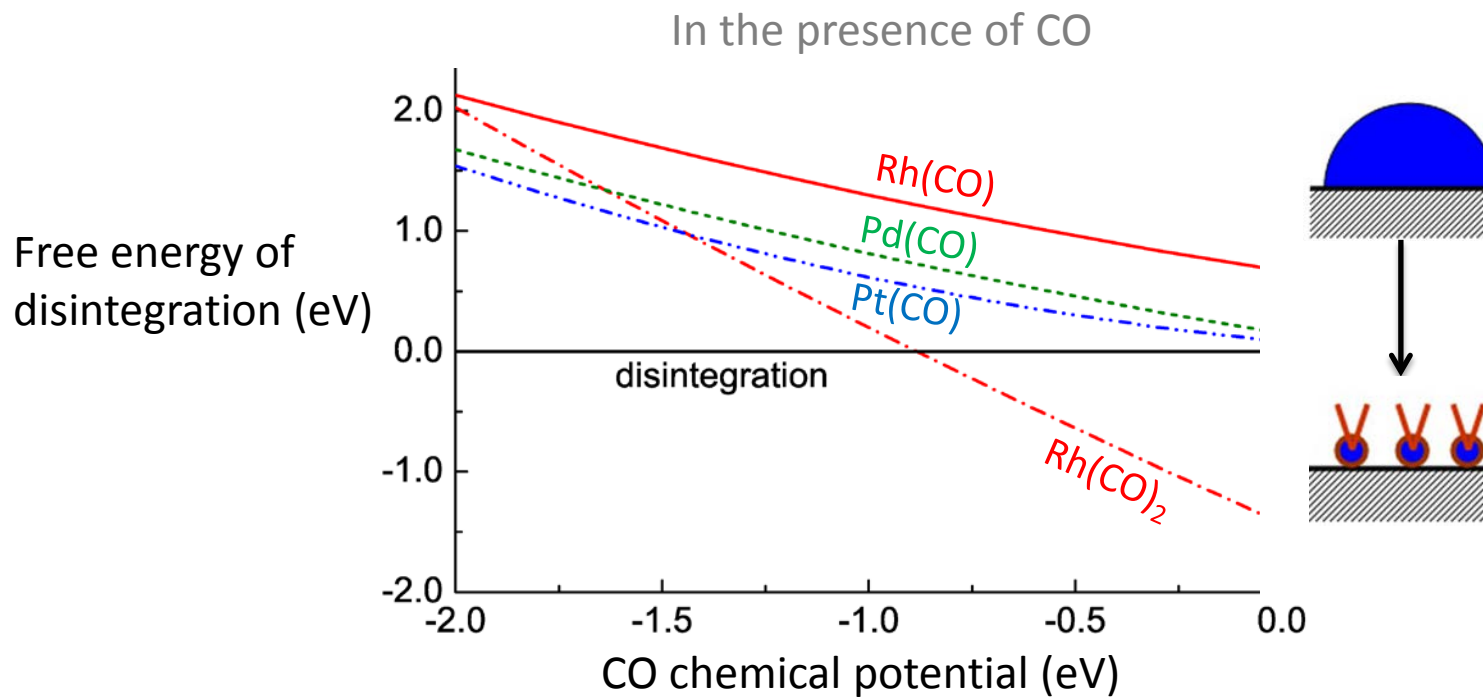
-1.58 eV

# Gas phase metal complexes not considered in disintegration analysis



- Higher order complexes also preferred gas phase
- These complexes not observed in experiments bound to support
- May play a role in gas phase ripening

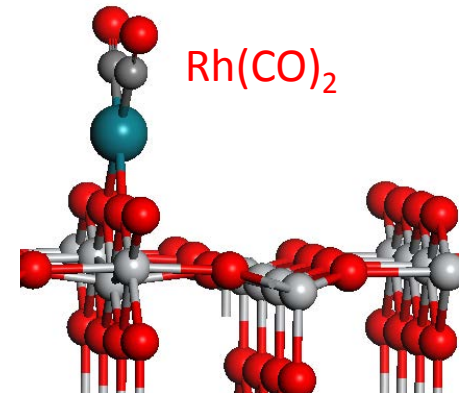
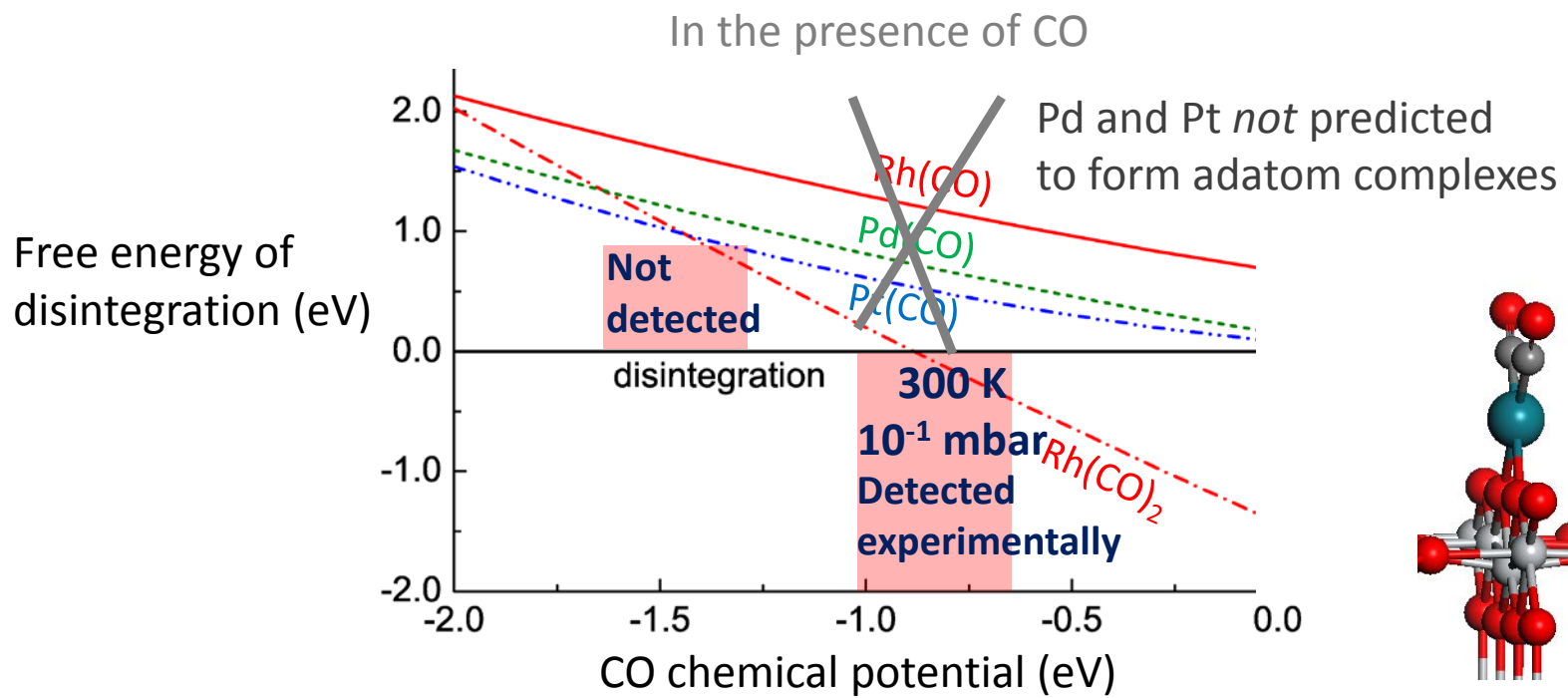
# Predicting particle disintegration under experimental conditions



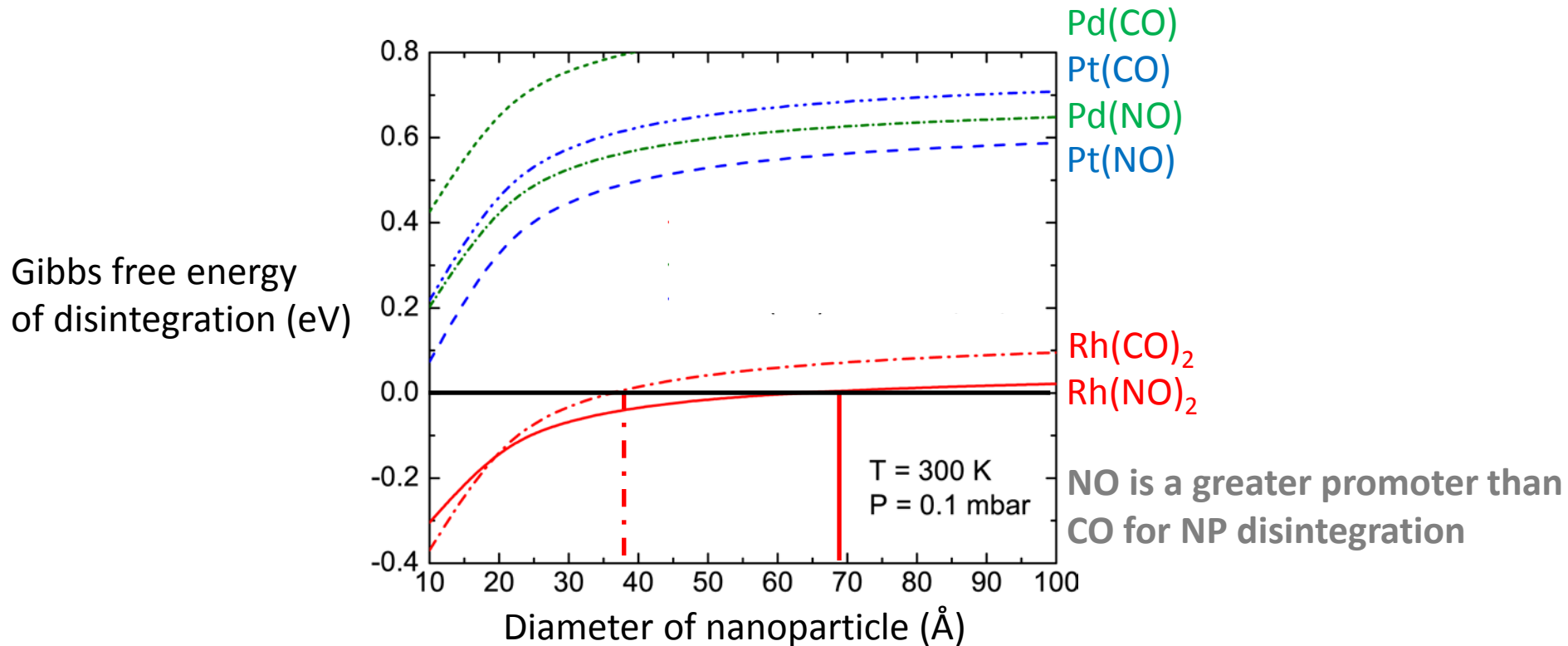
B. R. Goldsmith, E. D. Sanderson, R. Ouyang, W.-X. Li, J. Phys. Chem. C 118, 9588 (2014)

Ouyang et. al. J. Am. Chem. Soc. 135, 1760 (2013)

In agreement with experiment,  
 $\text{Rh}(\text{CO})_2$  predicted to form but not  $\text{Rh}(\text{CO})$



# Rh/TiO<sub>2</sub>(110) more responsive to CO and NO-induced disintegration than Pd or Pt

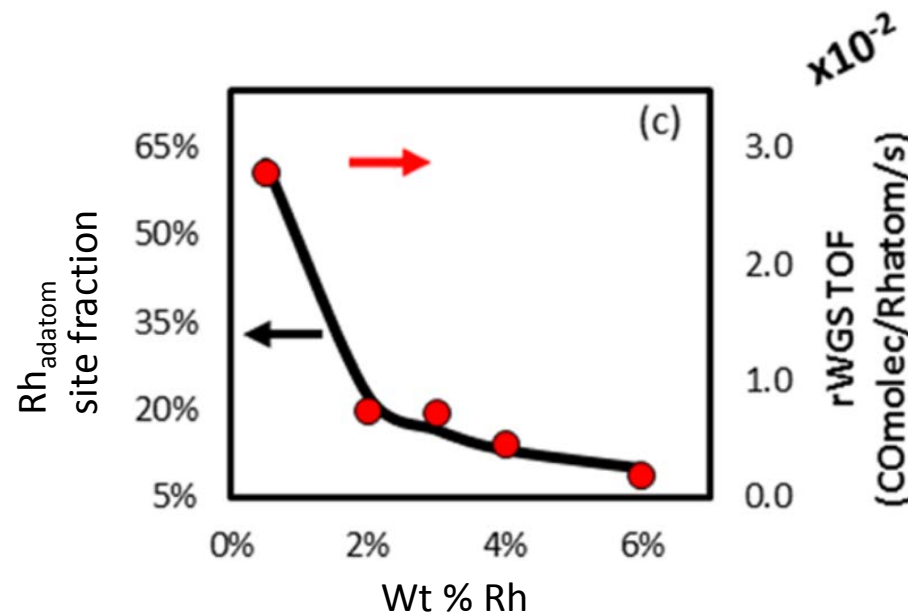
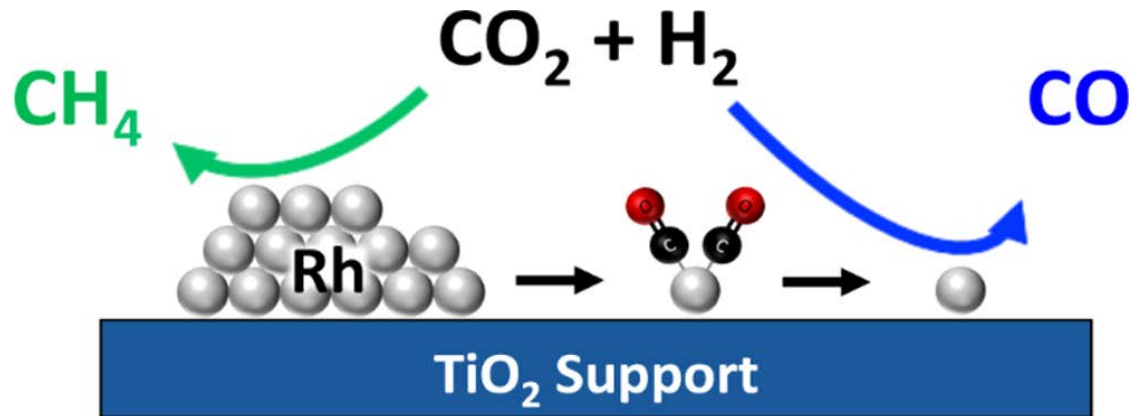


Experimentally<sup>[1]</sup> Rh(CO)<sub>2</sub>, d < 60 Å

Computed Rh(CO)<sub>2</sub>, d < 38 Å

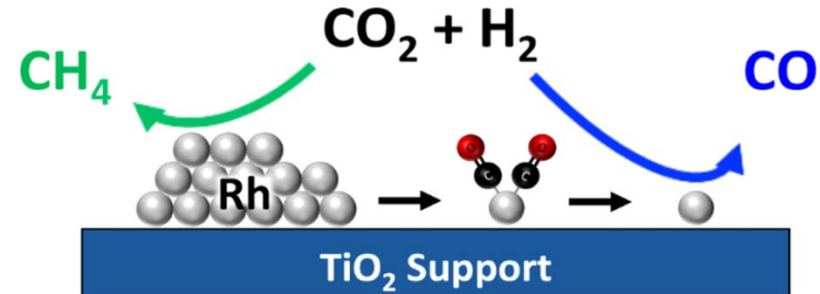
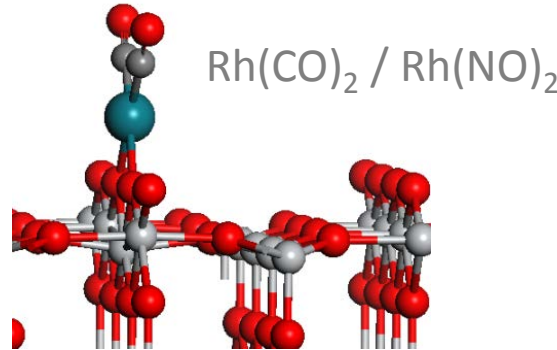
# Isolated Metal Active Site Concentration and Stability Control Catalytic CO<sub>2</sub> Reduction Selectivity

J. C. Matsubu, V. N. Yang, P. Christopher, J. Am. Chem. Soc , Just Accepted (2015)



# Nanoparticle disintegration can be predicted using *ab initio* thermodynamics

- Rh/TiO<sub>2</sub>(110) most susceptible to CO and NO-induced disintegration
- NO is a more efficient reactant for particle disintegration than CO
- Dominant driving force is adatom stabilization due to reactant binding

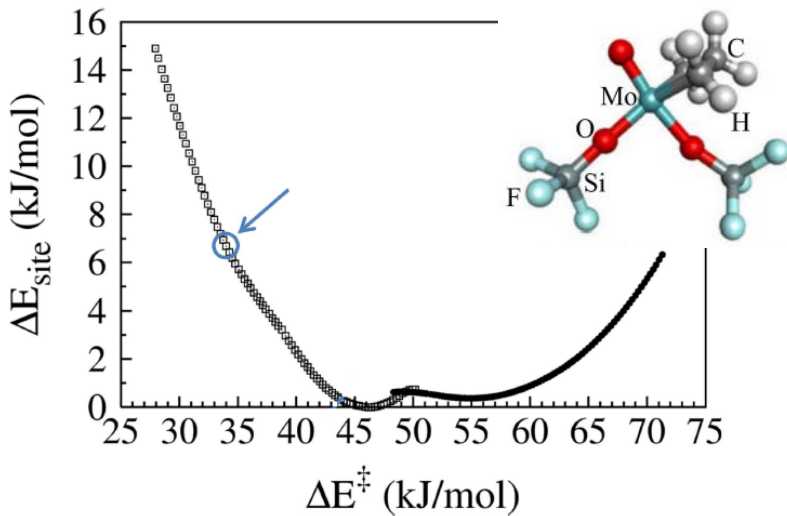


J. C. Matsubu, V. N. Yang, P. Christopher,  
J. Am. Chem. Soc., Just Accepted (2015)

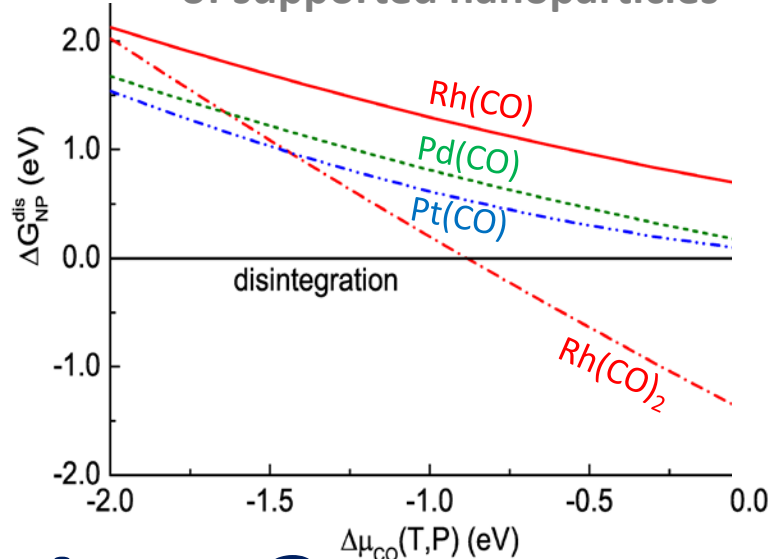
B. R. Goldsmith, E. D. Sanderson, R. Ouyang, W.-X. Li, J. Phys. Chem. C 118, 9588 (2014)  
R. Ouyang, J. X. Liu, W.-X. Li, J. Am. Chem. Soc. 135, 1760 (2013)

# Towards understanding the activity and stability of catalysts

Systematic algorithm to model isolated amorphous sites



Predicting the stability of supported nanoparticles



## Acknowledgements

Prof. Baron Peters

Prof. Susannah Scott

Prof. Wei-Xue Li

Dr. Runhai Ouyang

Evan D. Sanderson

Stefan Seritan

*All of my colleagues*

# Questions?



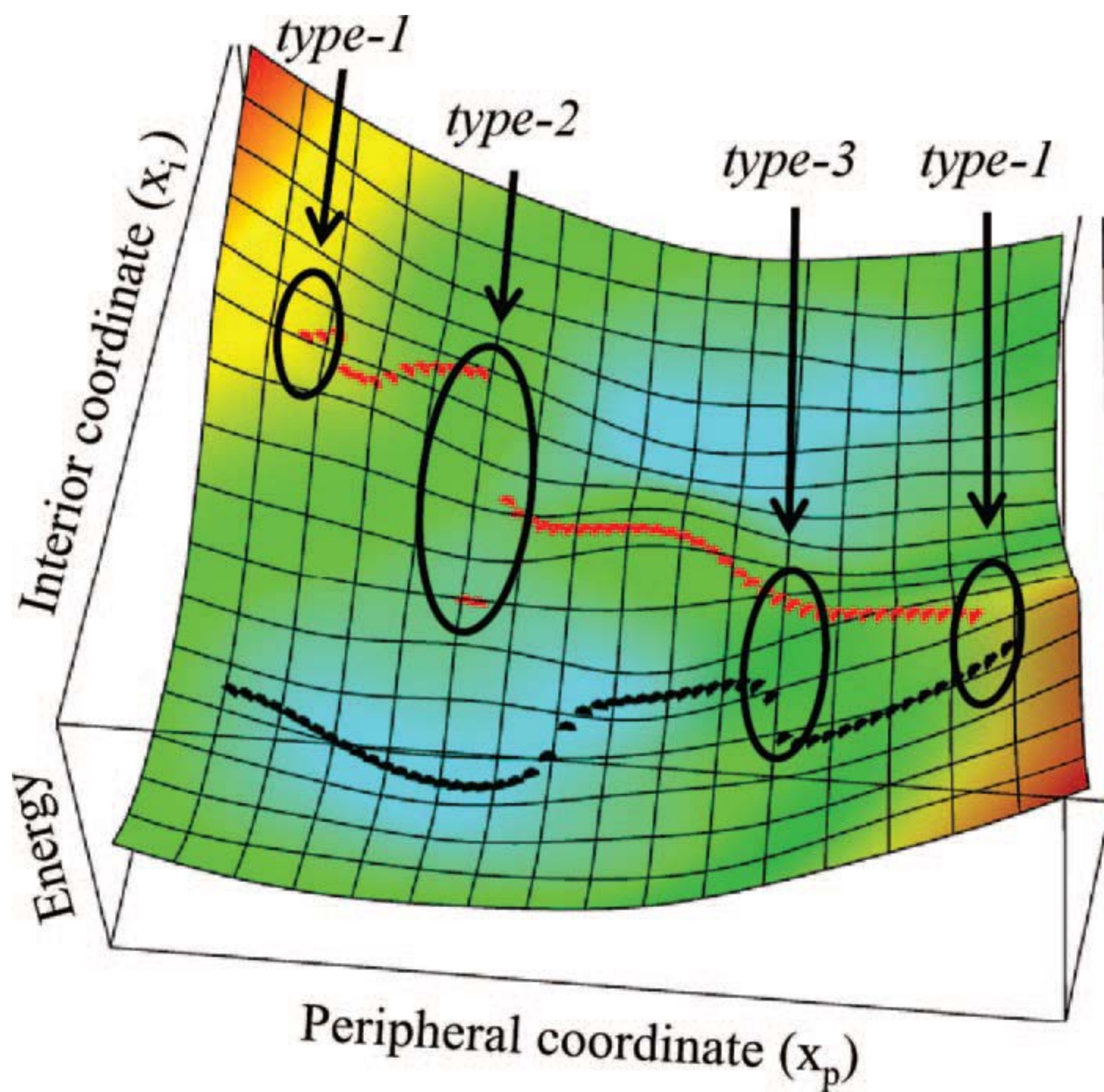
CHEMICAL ENGINEERING  
UC SANTA BARBARA



science crossing borders...

pire  
ccc  
i

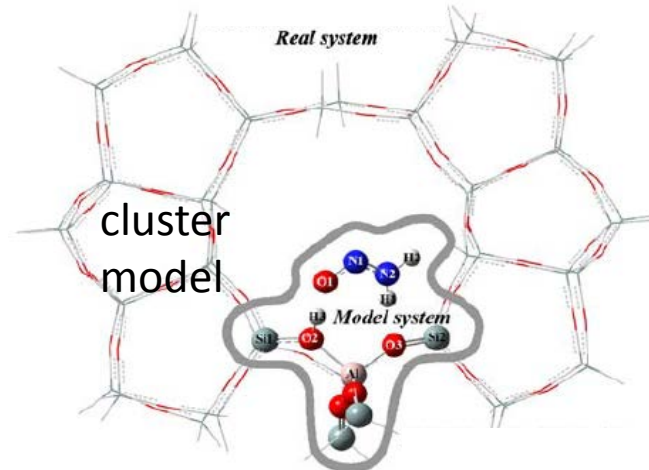
# Supporting Information



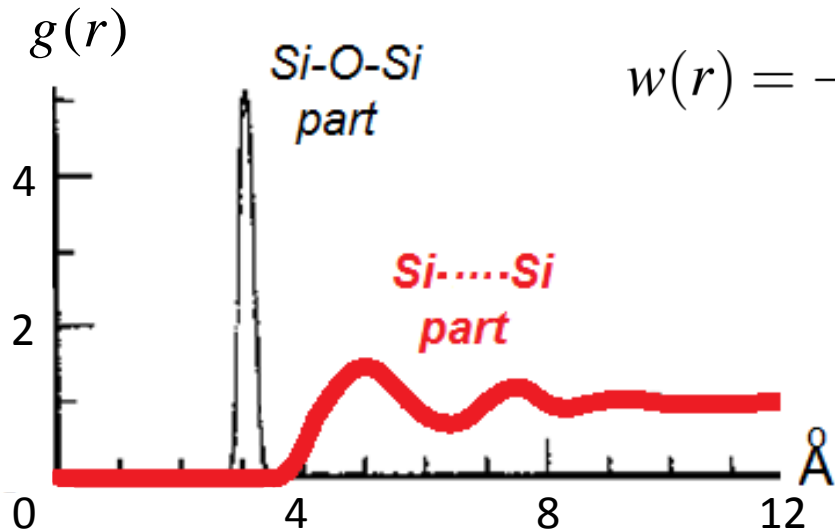
# Structural embedding

*Real site is embedded*, not isolated

- usually have electrostatic effects
- external matrix strain

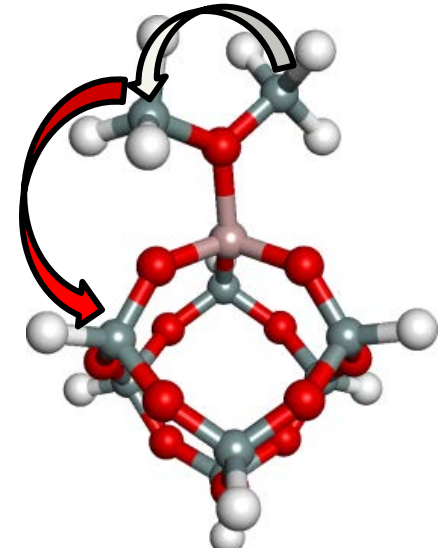


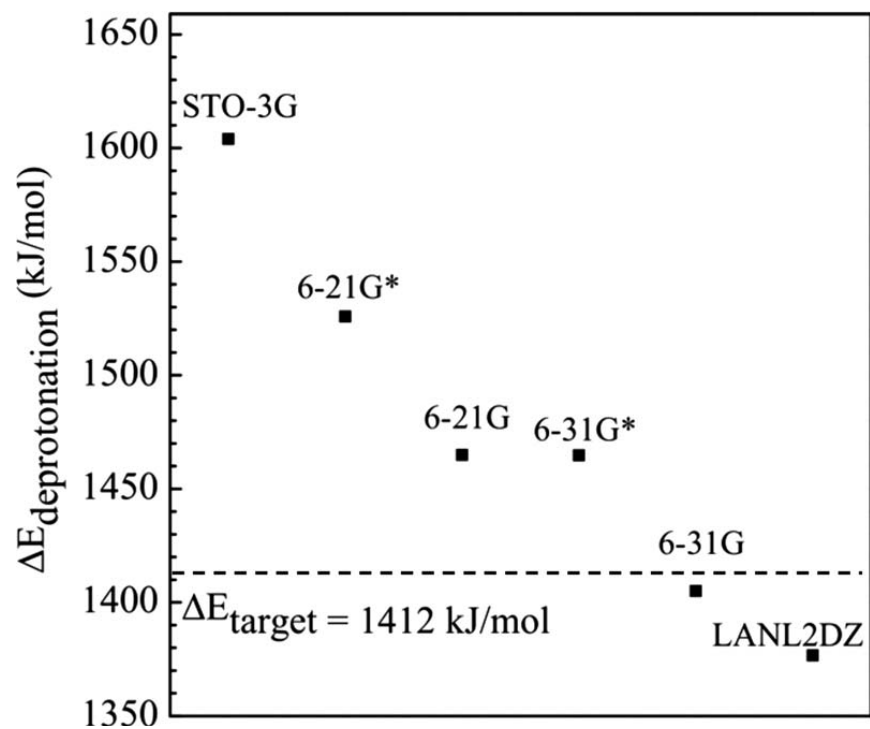
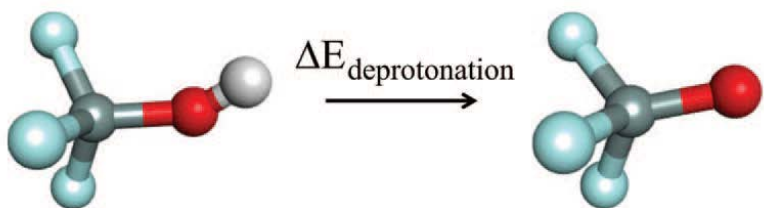
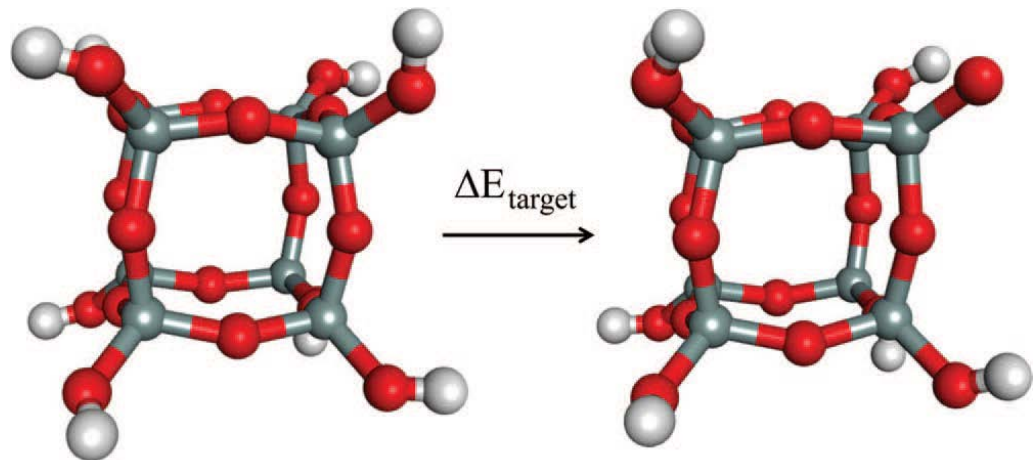
Bias the distribution of  $x_p$  pairs



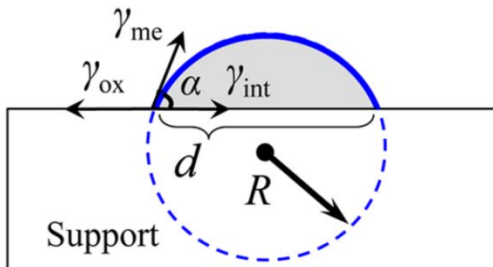
Si-O-Si:  
no need to modify

through-  
matrix forces





### Metal Particle



$\gamma_{me}$  is surface energy of metal particle

$\gamma_{int}$  is interfacial energy between metal particle and support

$\gamma_{ox}$  is surface energy of support

$H_{adh} = \gamma_{int} - \gamma_{me} - \gamma_{ox}$  is adhesion energy between metal particle and support  
 $\alpha$  is contact angle

### Exposed surface area of particle

$$A_s = 2\pi R^2 [1 - \cos(\alpha)] \quad \alpha = 90^\circ \rightarrow A_s = 2\pi R^2$$

$$\alpha = 180^\circ \rightarrow A_s = 4\pi R^2$$

Contact angle obtained via goniometry experiment

### Contact interface area between particle and support

$$A_{int} = \pi R^2 \sin^2(\alpha)$$

$$\alpha = 90^\circ \rightarrow A_{int} = \pi R^2$$

$$\alpha = 180^\circ \rightarrow A_{int} = 0$$

### Average energy $\Delta E_{NP}$ (per atom) with respect to infinite size particle (bulk)

$$\Delta E_{NP} = \frac{1}{N} [(A_s + A_{int}) \gamma_{me} + A_{int} H_{adh}]$$

$$N = \frac{4\pi R^3}{3} \left( \frac{\alpha_1}{\Omega} \right) = \text{Number of metal atoms in particle of interest}$$

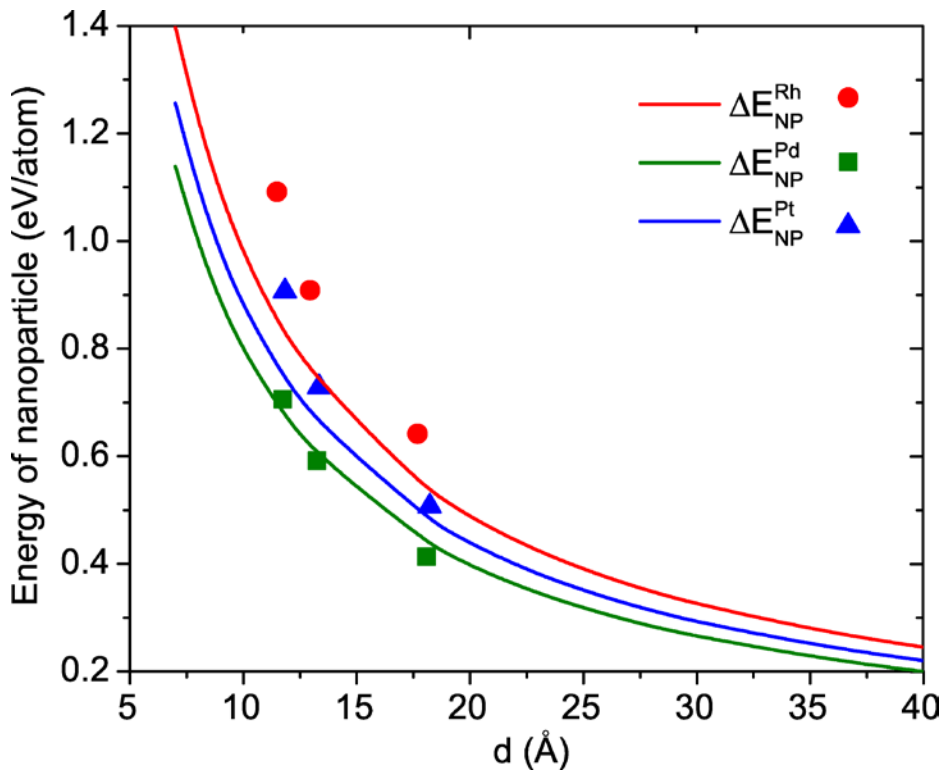
$$\alpha_1 = [2 - 3 \cos(\alpha) + \cos^3(\alpha)]/4$$

$$\Omega = \frac{4\pi r^3}{3\eta} = \text{Molar volume of bulk atom}$$

# Configurational Entropy

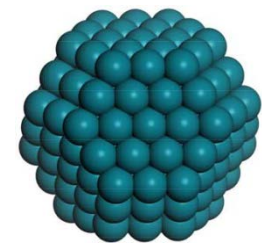
$$\begin{aligned}\Delta S &= \frac{k_B}{N} \ln \frac{N_t !}{N!(N_t - N)!} \\ &= -k_B \left[ \ln \theta_{mc} + \left( \frac{1}{\theta_{mc}} - 1 \right) \ln (1 - \theta_{mc}) + \frac{1}{N} \right] \\ &\approx -k_B \left[ \ln \theta_{mc} + \left( \frac{1}{\theta_{mc}} - 1 \right) \ln (1 - \theta_{mc}) \right]\end{aligned}$$

# Test approximation of constant surface energy vs. particle diameter



$$\Delta E_{NP} = \frac{3\Omega\gamma_{(111)}}{R} \text{ solid lines, constant } \gamma_{(111)}$$

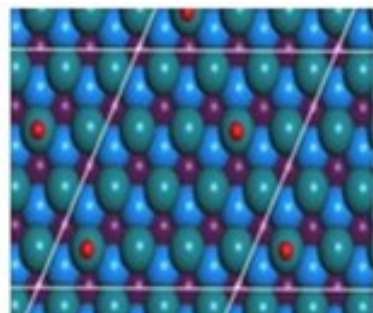
Solid points  
are nanoparticle  
energies via Wulff  
construction



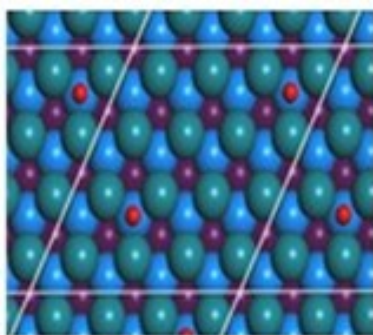
However,  $\gamma(R)$  should likely be used in kinetic studies.

Campbell, C. T.; P et al. *Science* 2002, 298, 811

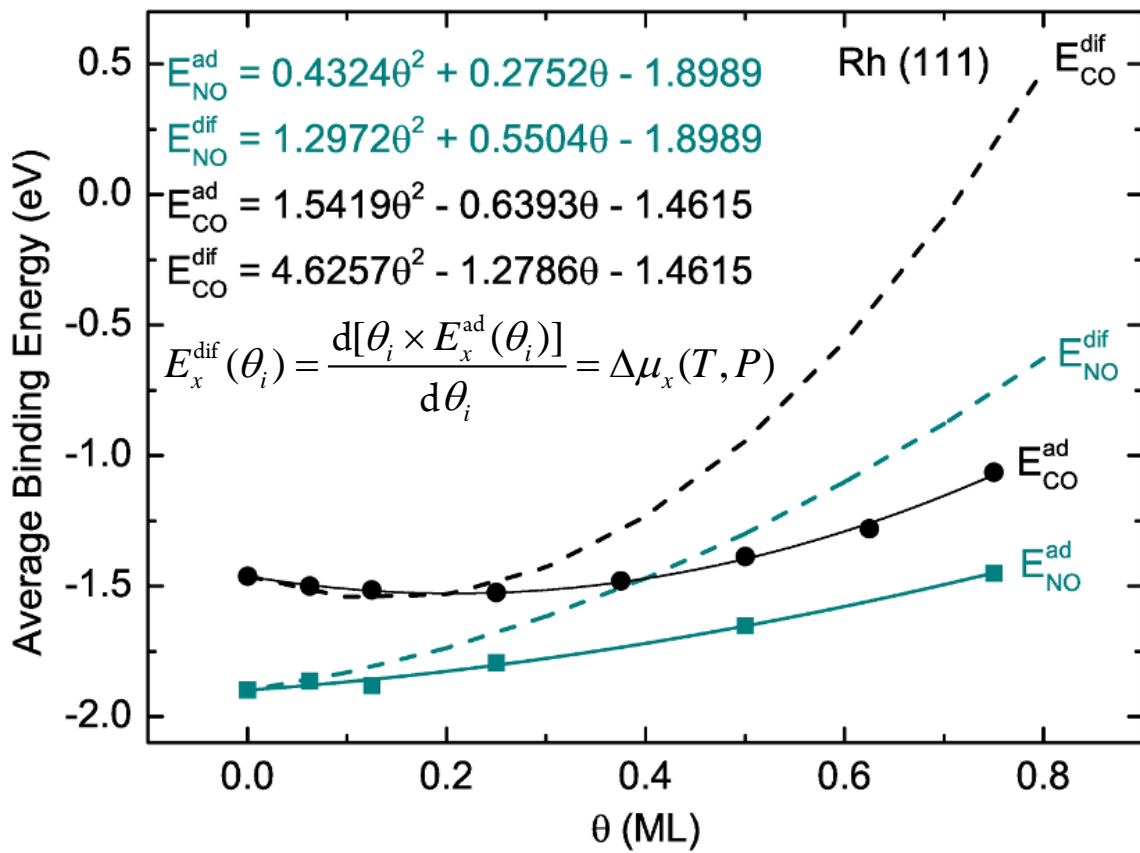
# Example: Coverage dependence of CO/NO binding on Rh (111) facet



0.125 ML, CO



0.125 ML, NO



Less pronounced difference between  
CO and NO binding for Pt and Pd

## NO adsorption positions

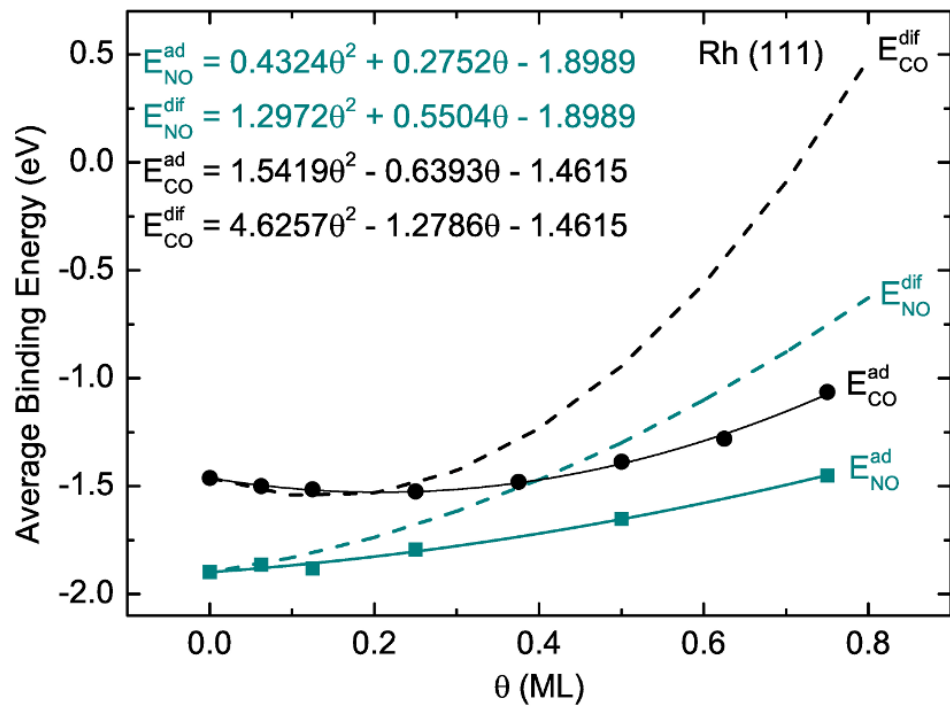
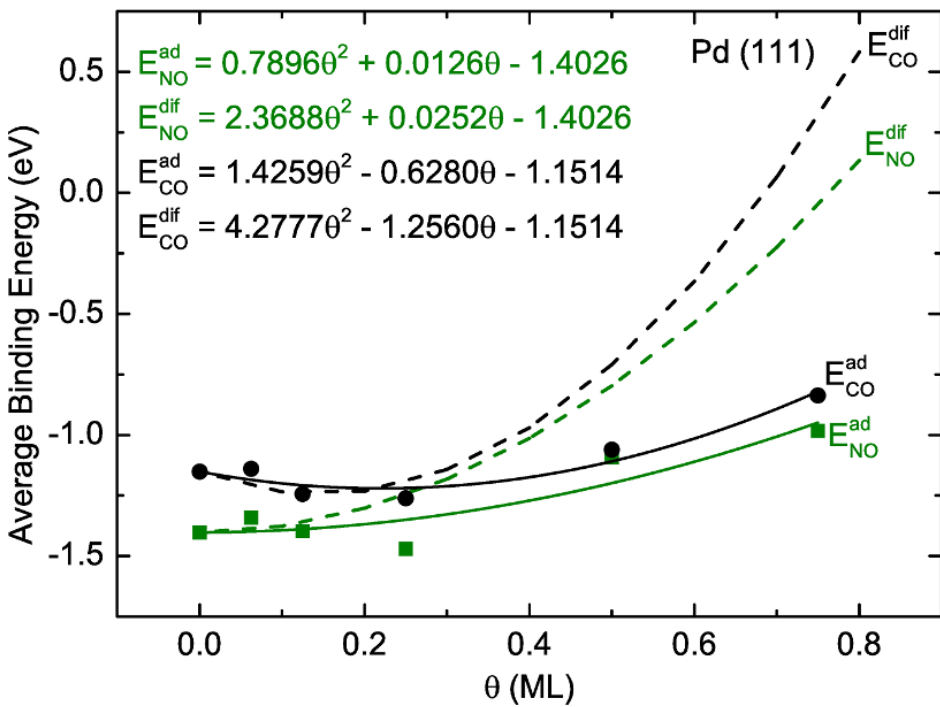
Zeng et al. Phys. Chem. Chem. Phys., 2010

## CO adsorption positions

R. Chen et al., Comput. Theor. Chem. 2011

$$\Delta\gamma_i(T, P) = \frac{\theta_i [E_x^{\text{ad}}(\theta_i) - \Delta\mu_x(T, P)]}{A_i}$$

# Surface coverage dependence of CO/NO binding on Pd, and Rh (111)



NO adsorption positions

Zeng et al. Phys. Chem. Chem. Phys., 2010.

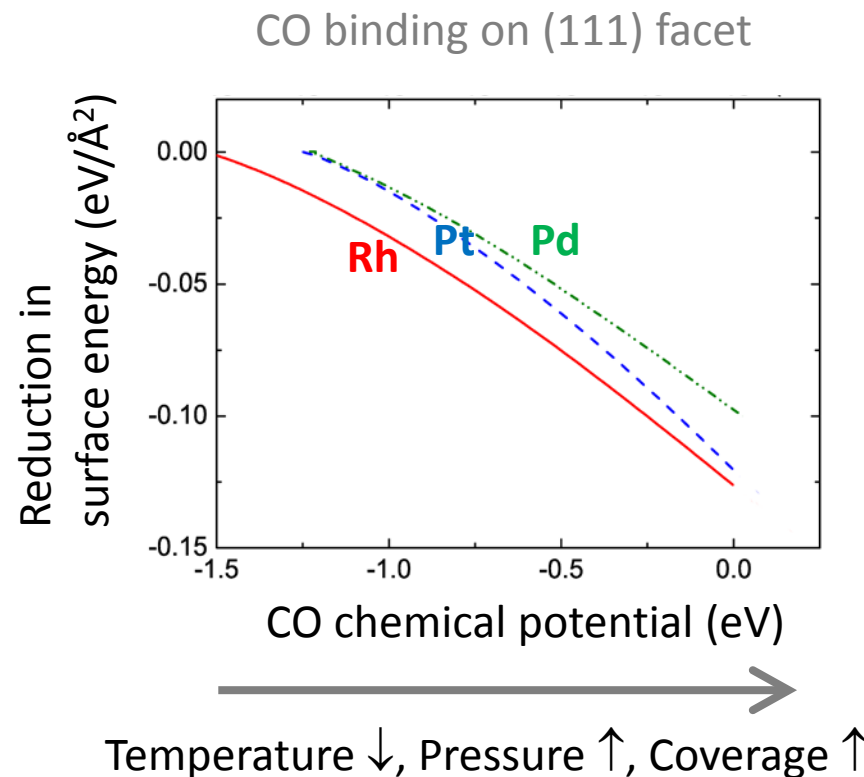
CO adsorption positions

R. Chen et al., Comput. Theor. Chem. 2011.

CO/NO bind strongest  
to Rh.  $[\text{d}^8 \text{ vs. } \text{d}^9]$

# Modeling reduction in surface energy due to reactant adsorption

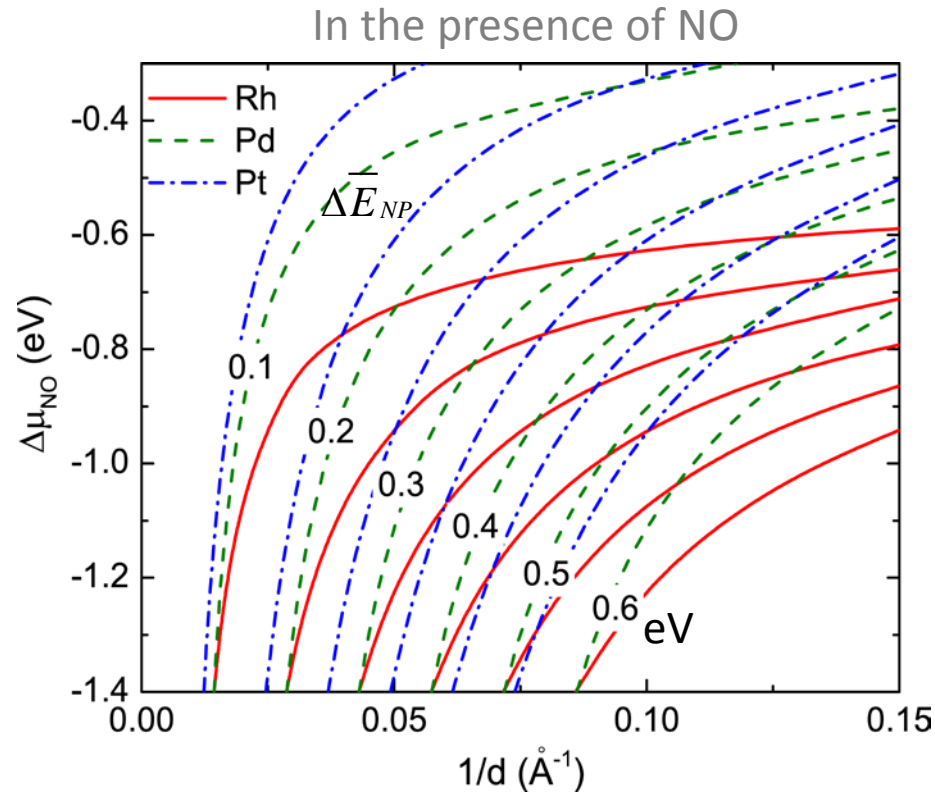
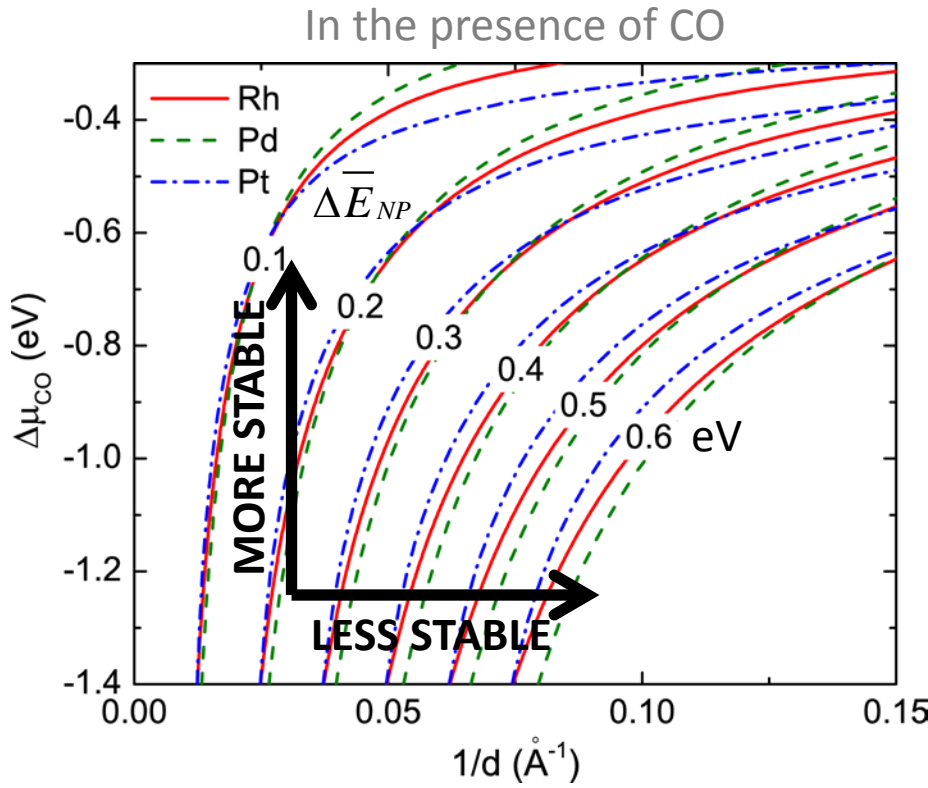
$$\bar{\gamma}_{me}(T, P) = \sum_i f_i [\gamma_i + \Delta\gamma_i(T, P)] \approx \gamma_{me}^{111} + \Delta\gamma_{me}^{111}(T, P)$$



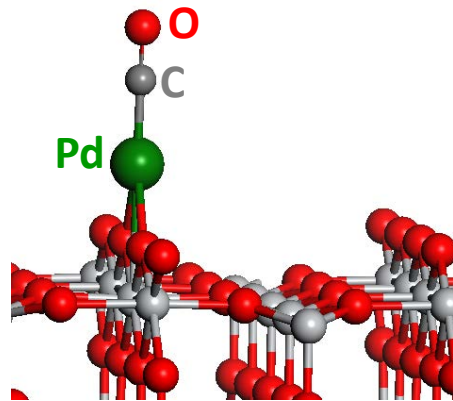
Based on differential binding energy calculations.

# Effects of chemical potential and particle size on particle energy

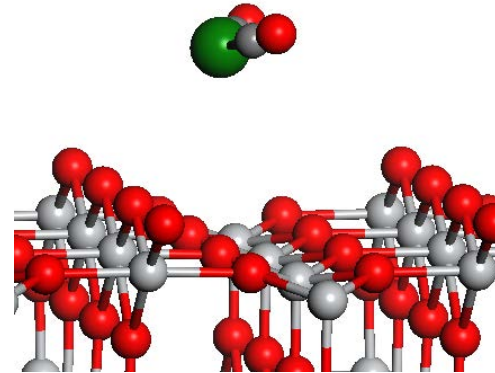
$$\Delta \bar{E}_{NP} = \frac{3\Omega \bar{\gamma}_{(111)}}{R} \text{ contours}$$



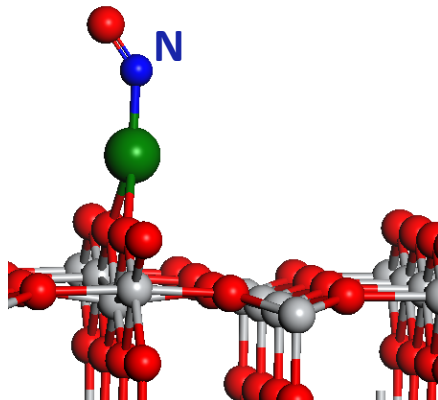
# CO/NO adsorption sites on Pd/TiO<sub>2</sub>(110)



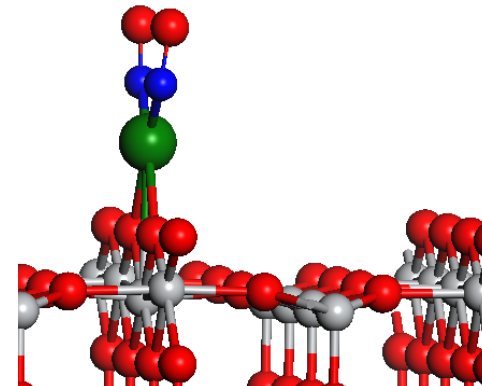
$$E_f^{\text{CO}} \text{ (mono)} = 0.26 \text{ eV}$$



$$E_f^{\text{CO}} \text{ (di)} = -0.54 \text{ eV}$$

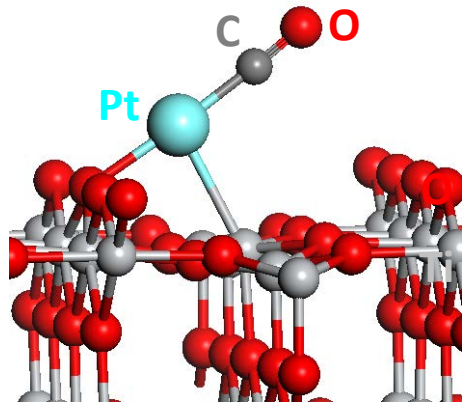


$$E_f^{\text{NO}} \text{ (mono)} = -0.05 \text{ eV}$$

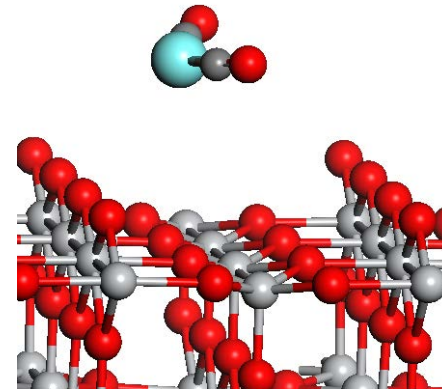


$$E_f^{\text{NO}} \text{ (di)} = -0.67 \text{ eV}$$

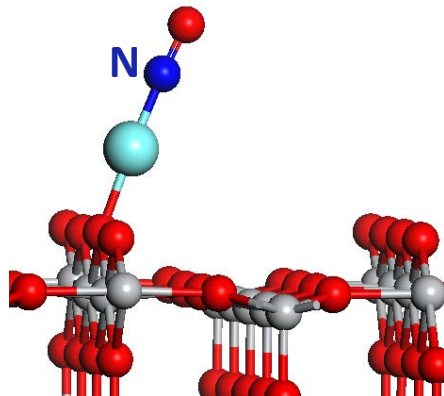
# CO/NO adsorption sites on Pt/TiO<sub>2</sub>(110)



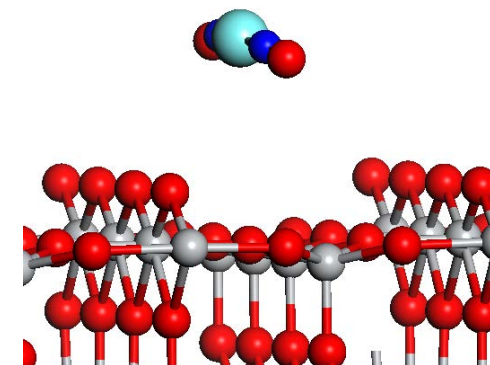
$$E_f^{\text{CO}} \text{ (mono)} = 0.09 \text{ eV}$$



$$E_f^{\text{CO}} \text{ (di)} = -0.69 \text{ eV}$$



$$E_f^{\text{NO}} \text{ (mono)} = -0.10 \text{ eV}$$



$$E_f^{\text{NO}} \text{ (di)} = -0.67 \text{ eV}$$

Also in agreement with experiment,  
 $\text{Rh}(\text{NO})_2$  predicted to form but not  $\text{Rh}(\text{NO})$

